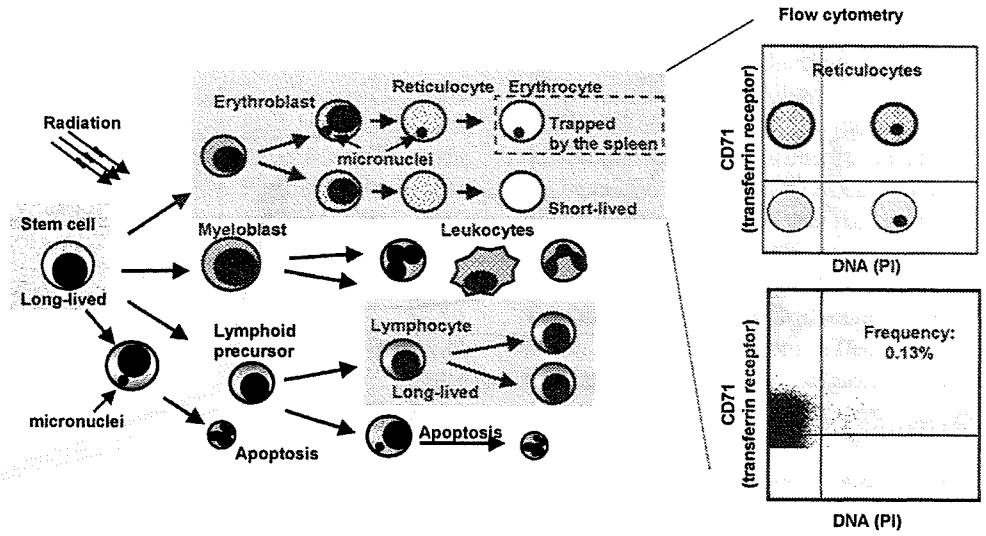

Fig. 3. A scheme of reticulocyte micronucleus assay thought to reflect the genetic damage involved in genetic instability induced by irradiation of the hematopoietic system. Circulating reticulocytes harboring micronuclei are differentiated from directly radiation-damaged precursor cells. Circulating reticulocytes with or without micronuclei will mature to erythrocytes in 3 days, resulting in elimination of directly damaged reticulocytes within a few days after irradiation. Therefore, micronuclei in reticulocytes after this acute phase are anticipated to indicate delayed radiation effects, namely genetic instability. The right panels show a schematic illustration of flow cytometry analysis of reticulocyte micronucleus and an actual flow cytometry pattern analyzing the reticulocyte micronucleus frequency in an irradiated mouse.

indication of genetic instability, is associated with the noted elevation of radiation-induced *GPA* Mf and with inflammatory status and ROS production in the survivors. Several flow cytometry methods measuring reticulocyte micronuclei in human blood samples have been developed [19,20]. Application of any one of these methods would allow us to further pursue molecular epidemiological investigations using this biomarker of genomic instability among the AHS population.

2.3. Biomarkers for inflammation and reactive oxygen species

Our immunology group has previously found that A-bomb radiation exposure enhanced persistent inflammation that is often accompanied with normal physiologic aging [5]. Further, inflammation-associated production of excessive levels of free radicals (e.g., ROS) is highly mutagenic. Therefore, endogenous ROS might be a factor to be analyzed with the aforementioned biomarkers. We have recently developed a total ROS assay system to determine the total amount of oxygen-centered free radicals derived from various ROS metabolites in a blood sample [21]. Our preliminary study showed that plasma ROS levels in AHS participants significantly increased with increased radiation dose (regression $P < 0.001$), even after adjustment was made for gender, age, smoking status and body mass (unpublished data).

3. Molecular oncology analyses of radiation-associated cancers

3.1. Adult-onset papillary thyroid cancer in the LSS cohort

Epidemiological studies on the LSS cohort of A-bomb survivors have identified a significant radiation-associated solid cancer risk [22]. However, the level of risk differed from organ to organ [22]. The excess relative risk of papillary thyroid cancer in survivors was 1.2 per Sv, and it increased with radiation dose [22]. A histopathological study has revealed that the thyroid cancer found in A-bomb survivors was largely conventional papillary in nature. This is also the case of spontaneous thyroid cancer in the Japanese at large. Solid variant papillary thyroid cancer was not found in A-bomb survivors, although this cancer has been frequently observed among post-Chernobyl children.

A major early event in papillary thyroid carcinogenesis is the constitutive activation of the MAP kinase signaling pathway caused by a single genetic alteration. This alteration has been identified as one among several possible, mutually exclusive, rearrangements of the *RET* and *NTRK-1* genes, and point mutations in the *RAS* and *BRAF* genes [23–25]. Among post-Chernobyl childhood thyroid cancers, the prevalent *RET/PTC3* rearrangement was closely associated with a short latency period after exposure and also with solid variant-type of the disease [26,27]. A low prevalence of *BRAF* mutation has been observed in childhood papillary thyroid cancer regardless of the presence or absence of past radiation exposure [28]. On the other hand, prevalence of *RET/PTC* rearrangements in radiation-associated adult-onset thyroid cancer, including radiation-therapy cases, was controversial [29,30]; *BRAF* point mutation ($BRAF^{V600E}$) was found at high frequency in papillary thyroid cancer among adult patients without history of radiation exposure [28]. In this regard, our previous experiments in vivo and in vitro showed that X-irradiation induced *RET/PTC1* rearrangement in scid mice within human thyroid tissue transplants, as well as in human thyroid cells cultured in vitro [31].

A logical first step for clarifying the mechanistic relationship between radiation exposure and the development of papillary thyroid cancer would be identification of the gene alterations that

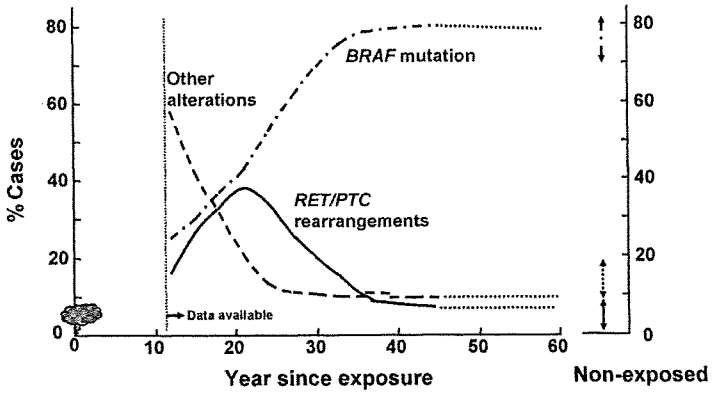

Fig. 4. A scheme of gene alteration types in adult-onset papillary thyroid cancer among A-bomb survivors varying with radiation dose and year elapsed since atomic radiation exposure.

preferentially occur during adult-onset radiation-associated thyroid carcinogenesis. Toward this end, we analyzed *RET/PTC* rearrangements and $BRAF^{V600E}$ point mutation among 50 adult-onset papillary thyroid cancer cases exposed to A-bomb radiation. Relationships to radiation dose, as well as years elapsed since A-bomb radiation exposure, were evaluated. When dividing the subjects into three groups harboring $BRAF^{V600E}$ mutation, *RET/PTC* rearrangements, and other unknown gene alterations, radiation dose (tertiles) responses of these groups differed: $BRAF^{V600E}$ mutation frequency significantly decreased in groups with increased radiation dose (Cochran-Armitage $P_{trend} < 0.001$) [6], while *RET/PTC* rearrangements showed significantly increased frequency with radiation dose (Cochran-Armitage $P_{trend} = 0.002$). Furthermore, other unknown gene alterations tended to be more frequent with increased radiation dose, suggesting that radiation-associated gene alterations (possible chromosomal rearrangements) other than *RET/PTC* rearrangements might be involved in the adult-onset thyroid cancers of A-bomb survivors who were exposed to high radiation doses. These findings also correspond with another significant observation in the same subjects: namely that the subjects with *RET/PTC* rearrangements developed cancer sooner following exposure than did the subjects with $BRAF^{V600E}$ mutation, as illustrated in Fig. 4 (Mann–Whitney, $P = 0.029$). Together, the interim results obtained thus far suggest an important role of *RET/PTC* rearrangements in adult-onset radiation-associated thyroid carcinogenesis.

3.2. Colorectal cancer from the LSS cohort

Radiation exposure was associated with increased risk of colon cancer (excess relative risk per Sv of 0.72, 95% confidence interval 0.29–1.28); interestingly, rectal cancer did not show apparent risk elevation upon radiation exposure [22]. In colorectal cancer, two major phenotypes, i.e., chromosomal instability and microsatellite instability (MSI), were correlated with different subsites of the colorectum. Specifically, high-MSI (MSI-H) cancer was frequently found at a specific subsite—the proximal colon [32]. Therefore, we hypothesized that the MSI phenotype might be associated with radiation exposure.

First, we determined MSI status in 24 colon and 11 rectal cancers in A-bomb survivors with defined radiation doses, in terms of six microsatellite markers. Five MSI-H cases were found among them, all in the proximal colon and none in the rectum. The median radiation dose of MSI-H colorectal cancer patients was significantly higher than that of microsatellite stable (MSS) and low-MSI (MSI-L) cancer patients (Mann–Whitney, $P = 0.042$). These observations suggest a possible link between radiation exposure and MSI.

Most MSI-H sporadic colorectal cancers showed loss of expression of the MLH1 DNA repair enzyme and the methylation of its promoter. The latter is probably a major cause for inactivation of this gene [33]. We examined as well the methylation of the CpG dinucleotides within the proximal region (−231 to −228) of the *MLH1* gene, since this CpG island is responsible for decreased mRNA and/or protein expression of the gene [34–36]. Using combined bisulfite restriction analysis [37], methylation of the *MLH1* gene was found in five patients, whose median radiation dose tend to be higher than that of subjects with *MLH1*-unmethylated genes; this finding, however, is of marginal significance (Mann–Whitney, $P = 0.06$). Methylation of the *MLH1* gene was significantly associated with MSI status in this study (χ^2, $P = 0.017$), as was the case in other studies: three patients showed both methylation of the *MLH1* gene and the MSI-H phenotype.

In addition to DNA methylation, we examined loss-of-heterozygosity (LOH) of the *MLH1* gene, which is also responsible for deficient expression of the *MLH1* gene [33]. We found that all five MSI-H cases carried LOH at the gene loci. Our preliminary findings imply that MSI colorectal carcinogenesis among A-bomb survivors might involve both epigenetic and genetic alterations of the *MLH1* gene.

During the past decade, it has become clear that there is a "serrated polyp pathway" associated with MSI [38]. This pathway is initiated by hyperplastic polyp formation, followed by serrated adenoma, and ultimately leading to invasive cancer. Loss of the MLH1 protein followed by acquisition of MSI occurs at the late stage [39], while point mutation of the *BRAF* gene ($BRAF^{V600E}$) is recognized as an early event [40]. We therefore examined $BRAF^{V600E}$ and found that four cases possessed this mutation. The median radiation dose of

BRAF-mutated cases was significantly higher than that of non-mutated cases.

Our results to date suggest that radiation exposure might influence MSI status through MSI-related epigenetic and genetic alterations—processes that may have occurred in the early stage of colorectal carcinogenesis. Further analysis with an increased number of cases is clearly required, however.

4. Future directions

Epidemiological follow-up study among A-bomb survivors for over half a century has provided invaluable knowledge about how atomic-radiation influenced disease outcome, and it will continue to do so in the years ahead. However, relatively little is known about the mechanisms of adverse health effects of ionizing radiation that arise late in life. For example, risk of various solid cancers increased with radiation dose and remain high, despite six decades since the exposure event. We still do not know why some organs are more sensitive to radiation exposure than others, and why cancer incidence within such organs remains high. Apart from determining risk for the population at large, a more elusive question is how to evaluate individual sensitivity to various radiation effects and how to handle risk estimation of individuals. The molecular epidemiology study at RERF seeks to find the answers to these important questions relating to the health effects of radiation.

It may be noted that the primary aim of molecular epidemiology is not necessarily to find association between radiation and disease outcome, but to assess the various radiation effects on cells, tissues, organs, and vital physiological systems and processes of the body, such as immunity and DNA repair, in terms of various biomarkers, some of which may be related to disease. The biomarkers to be used in our somatic mutability and molecular oncology studies are listed in Table 1, together with possible use of stored biological materials. Our somatic mutability study is positioned to look at the systemic effects of radiation. In fact, the observed relationship between *GPA* Mf, radiation dose, and solid cancers suggests that atomic radiation might exert long-lasting and systemic effects on the mutability of tissue cells of the body and not exclusively of hematopoietic cells, since increased *GPA* Mf at high doses was closely associated with cancers of various organs and not just the hematopoietic system. We anticipate that the results of the γH2AX and reticulocyte micronucleus assays will deepen our mechanistic understanding of radiation-induced somatic mutability.

Nevertheless, we still are looking at only the "shadow" of radiation effects. This is due, in part, to the fact that our survey has been and will continue to be performed well over 40 years after the bombings, and that the direct targets of radiation are stem/progenitor cells, the nature of which generally differs from that of differentiated cells. In the future, somatic mutability studies need to combine with stem cell biology studies, so that radiation effects on stem cells and early progenitors can be investigated in terms of genetic and epigenetic alterations, stem cell senescence, and genome maintenance.

Carcinogenic pathways appear to differ significantly between organ systems and specific types of pathologies, as evidenced by the markedly different cancer risks in various organs of the A-bomb survivors. Only a few molecular oncology studies on cancers among A-bomb survivors have been reported in the past. This is due in part to the difficulty in collecting cancer tissue samples as well as the difficulty in analyzing those long-term preserved formalin-fixed samples at the molecular level. As a result of our molecular oncology study, sophisticated methods have been developed for the analyses of archived, often decades old, tissue samples [41], and have examined the molecular events in the carcinogenic pathways of particular cancers, as influenced by radiation exposure. Results of our adult-onset papillary thyroid and colorectal cancer studies have suggested that radiation did not alter basic pathways, but preferentially induced specific events: e.g., preferential occurrence of chromosome aberrations in the early stage of papillary thyroid carcinogenesis, and MSI and its related molecular events as consequences, not causes, of colorectal carcinogenesis. Although sufficiently intense ionizing irradiation may be associated with genome-wide hypomethylation, comparable irradiation might be related to hypermethylation of specific genes. This may be the case in *MLH1* hypermethylation in colorectal cancer.

Our findings on thyroid and colorectal cancers remain preliminary. Given the potential implications of our preliminary findings, further work is warranted to assess more thoroughly the mechanisms of radiation-associated cancer. To pursue these molecular oncology studies, cancer tissue samples from

Table 1
The biomarkers to be used for RERF somatic mutability and molecular oncology studies

Biomarkers	Materials (other than fresh samples)	Related functions/phenotypes
GPA Mf	Paraformaldehyde- or DMS-fixed blood cells	Somatic mutability
γH2AX foci	Cultured T-lymphocytes (expanded from cryopreserved uncultured ones)	Radiation sensitivity
Reticulocyte micronuclei	Methanol-fixed blood cells	Acute and delayed genetic damage
Total ROS metabolites	Frozen serum or plasma	Cumulated ROS
RET rearrangements and *BRAF* mutation (papillary thyroid cancer)	Long-term preserved paraffin blocks	Chromosome aberration vs. point mutation, relative to radiation effects
MSI-related events (colorectal cancer)	Long-term preserved paraffin blocks	Microsatellite unstable carcinogenesis
MLH1 gene methylation		
Alterations in Ras signaling		

A-bomb survivors, which are precious but presently spread over many hospitals, need to be collected in greater number and with greater efficiency.

We anticipate that our study will be linked to "molecular event-based risk estimation" of radiation-associated cancers, where the dose-risk relationships will be evaluated not only for a particular cancer-site but also for the fraction of this cancer harboring a specific molecular alteration, for example, radiation-induced risk of papillary thyroid cancer with *RET/PTC* rearrangements and MSI-positive colorectal cancer. These data will contribute not only to the mechanistic understanding of radiation-associated cancers but also to the future prevention of these cancers associated with natural, medical, occupational, and accidental exposure to radiation.

Acknowledgements

The Radiation Effects Research Foundation is a private non-profit foundation funded equally by the Japanese Ministry of Health, Labour and Welfare and the U.S. Department of Energy, the latter through the National Academy of Sciences. This study is in part supported by Grant-in-Aid for Scientific Research from the Ministry of Education, Culture, Sports, Science, and Technology of Japan and Grant-in-Aid for Cancer Research from the Ministry of Health, Labour and Welfare of Japan. This publication was based on RERF Research Protocols RP3-87, RP1-93, RP5-02, B38-04 and B44-06.

References

[1] Y. Kusunoki, T. Hayashi, Long-lasting alterations of the immune system by ionizing radiation exposure: implications for disease development among atomic bomb survivors, Int. J. Radiat. Biol. 84 (2007) 1–14.

[2] S. Kyoizumi, Y. Kusunoki, T. Hayashi, M. Hakoda, J.B. Cologne, K. Nakachi, Individual variation of somatic gene mutability in relation to cancer susceptibility: prospective study on erythrocyte glycophorin A gene mutations of atomic bomb survivors, Cancer Res. 65 (2005) 5462–5469.

[3] K. Hamasaki, K. Imai, K. Nakachi, N. Takahashi, Y. Kodama, Y. Kusunoki, Short-term culture and γH2AX flow cytometry determine differences in individual radiosensitivity in human peripheral T lymphocytes, Environ. Mol. Mutagen. 48 (2007) 38–47.

[4] K. Hamasaki, K. Imai, T. Hayashi, K. Nakachi, Y. Kusunoki, Radiation sensitivity and genomic instability in the hematopoietic system: frequencies of micronucleated reticulocytes in whole-body X-irradiated BALB/c and C57BL/6 mice, Cancer Sci. 98 (2007) 1840–1844.

[5] T. Hayashi, Y. Morishita, Y. Kubo, Y. Kusunoki, I. Hayashi, F. Kasagi, M. Hakoda, S. Kyoizumi, K. Nakachi, Long-term effects of radiation dose on inflammatory markers in atomic bomb survivors, Am. J. Med. 118 (2005) 83–86.

[6] K. Takahashi, H. Eguchi, K. Arihiro, R. Ito, K. Koyama, M. Soda, J.B. Cologne, Y. Hayashi, K. Nakachi, K. Hamatani, The presence of *BRAF* point mutation in adult papillary thyroid carcinomas from atomic bomb survivors correlates with radiation dose, Mol. Carcinogenesis 46 (2007) 242–248.

[7] S. Kyoizumi, M. Akiyama, J.B. Cologne, K. Tanabe, N. Nakamura, A.A. Awa, Y. Hirai, Y. Kusunoki, S. Umeki, Somatic cell mutations at the glycophorin A locus in erythrocytes of atomic-bomb survivors: implications for radiation carcinogenesis, Radiat. Res. 146 (1996) 43–52.

[8] S. Kyoizumi, N. Nakamura, M. Hakoda, A.A. Awa, M.A. Bean, R.H. Jensen, M. Akiyama, Detection of somatic mutations at the glycophorin A locus in erythrocytes of atomic bomb survivors using a single beam flow sorter, Cancer Res. 49 (1989) 581–588.

[9] E.P. Rogakou, D.R. Pilch, A.H. Orr, V.S. Ivanova, W.M. Bonner, DNA double-stranded breaks induce histone H2AX phosphorylation on serine 139, J. Biol. Chem. 273 (1998) 5858–5868.

[10] E.P. Rogakou, C. Boon, C. Redon, W.M. Bonner, Megabase chromatin domains involved in DNA double-strand breaks *in vivo*, J. Cell Biol. 146 (1999) 905–916.

[11] A. Takahashi, T. Ohnishi, Does γH2AX foci formation depend on the presence of DNA double strand breaks? Cancer Lett. 229 (2005) 171–179.

[12] Y. Ichijima, R. Sakasai, N. Okita, K. Asahina, S. Mizutani, H. Teraoka, Phosphorylation of histone H2AX at M phase in human cells without DNA damage response, Biochem. Biophys. Res. Commun. 336 (2005) 807–812.

[13] K.J. McManus, M.J. Hendzel, ATM-dependent DNA damage-independent mitotic phosphorylation of H2AX in normally growing mammalian cells, Mol. Biol. Cell 16 (2005) 5013–5025.

[14] S.A. Lorimore, P.J. Coates, E.G. Wright, Radiation-induced genomic instability and bystander effects: inter-related nontargeted effects of exposure to ionizing radiation, Oncogene 22 (2003) 7058–7069.

[15] J. Grawe, G. Zetterberg, H. Amneus, Flow-cytometric enumeration of micronucleated polychromatic erythrocytes in mouse peripheral blood, Cytometry 13 (1992) 750–758.

[16] S.D. Dertinger, D.K. Torous, K.R. Tometsko, Simple and reliable enumeration of micronucleated reticulocytes with a single-laser flow cytometer, Mutat. Res. 371 (1996) 283–292.

[17] N. Asano, Y. Katsuma, H. Tamura, N. Higashikuni, M. Hayashi, An automated new technique for scoring the rodent micronucleus assay: computerized image analysis of acridine orange supravitally stained peripheral blood cells, Mutat. Res. 404 (1998) 149–154.

[18] W. Krzyzanski, J.J. Perez-Ruixo, An assessment of recombinant human erythropoietin effect on reticulocyte production rate and lifespan distribution in healthy subjects, Pharm. Res. 24 (2007) 758–772.

[19] J. Grawe, J. Biko, R. Lorenz, C. Reiners, H. Stopper, S. Vershenya, V. Vukicevic, K. Hempel, Evaluation of the reticulocyte micronucleus assay in patients treated with radioiodine for thyroid cancer, Mutat. Res. 583 (2005) 12–25.

[20] S.D. Dertinger, R.K. Miller, K. Brewer, T. Smudzin, D.K. Torous, D.J. Roberts, S.L. Avlasevich, S.M. Bryce, S. Sugunan, Y. Chen, Automated human blood micronucleated reticulocyte measurements for rapid assessment of chromosomal damage, Mutat. Res. 626 (2007) 111–119.

[21] I. Hayashi, Y. Morishita, K. Imai, M. Nakamura, K. Nakachi, T. Hayashi, High-throughput spectrophotometric assay of reactive oxygen species in serum, Mutat. Res. 631 (2007) 55–61.

[22] D.E. Thompson, K. Mabuchi, E. Ron, M. Soda, M. Tokunaga, S. Ochikubo, S. Sugimoto, T. Ikeda, M. Terasaki, S. Izumi, D.L. Preston, Cancer incidence in atomic bomb survivors. Part II: Solid tumors, 1958–1987, Radiat. Res. 137 (1994) S17–S67.

[23] E.T. Kimura, M.N. Nikiforova, Z. Zhu, J.A. Knauf, Y.E. Nikiforov, J.A. Fagin, High prevalence of BRAF mutations in thyroid cancer: genetic evidence of constitutive activation of the RET/PTC-RAS-BRAF signaling pathway in papillary thyroid carcinoma, Cancer Res. 63 (2003) 1454–1457.

[24] P. Soares, V. Trovisco, A.S. Rocha, J. Lima, P. Castro, A. Preto, V. Maximo, T. Botelho, R. Seruca, M. Sobrinho-Simoes, BRAF mutations and RET/PTC rearrangements are alternative events in the etiopathologenesis of PTC, Oncogene 22 (2003) 4578–4580.

[25] M. Frattini, C. Ferrario, P. Bressan, D. Balestra, L. De Cecco, P. Mondellini, I. Bongarzone, P. Collini, M. Gariboldi, S. Pilotti, M.A. Pierotti, A. Greco, Alternative mutations of *BRAF, RET* and *NTRK1* are associated with similar but distinct gene expression patterns in papillary thyroid cancer, Oncogene 23 (2004) 7436–7440.

[26] Y.E. Nikiforov, J.M. Rowland, K.E. Bove, H. Monforte-Munoz, J.A. Fagin, Distinct pattern of ret oncogene rearrangements in morphological variants of radiation-induced and sporadic thyroid papillary carcinomas in children, Cancer Res. 57 (1997) 1690–1694.

[27] H.M. Rabes, E.P. Demidchik, J.D. Sidorow, E. Lengfelder, C. Beimfohr, D. Hoelzel, S. Klugbauer, Pattern of radiation-induced RET and NTRK1 rearrangements in 191 post-Chernobyl papillary thyroid carcinomas: biological, phenotypic, and clinical implications, Clin. Cancer Res. 6 (2000) 1093–1103.

[28] M. Xing, *BRAF* mutation in thyroid cancer, Endocr. Related Cancer 12 (2005) 245–262.
[29] A. Bounacer, R. Wicker, B. Caillou, A.F. Cailleux, A. Sarasin, M. Schlumberger, H.G. Suarez, High prevalence of activating *ret* proto-oncogene rearrangements, in thyroid tumors from patients who had received external radiation, Oncogene 15 (1997) 1263–1273.
[30] R. Elisei, C. Romei, T. Vorontsova, B. Cosci, V. Veremeychik, E. Kuchinskaya, F. Basolo, E.P. Demidchik, P. Miccoli, A. Pinchera, F. Pacini, RET/PTC rearrangements in thyroid nodules: studies in irradiated and not irradiated, malignant and benign thyroid lesions in children and adults, J. Clin. Endocrin. Metabol. 86 (2001) 3211–3216.
[31] T. Mizuno, K.S. Iwamoto, S. Kyoizumi, H. Nagamura, T. Shinohara, K. Koyama, T. Seyama, K. Hamatani, Preferential induction of RET/PTC1 rearrangement by X-ray irradiation, Oncogene 19 (2000) 438–443.
[32] K. Soreide, E.A. Janssen, H. Soiland, H. Korner, J.P. Baak, Microsatellite instability in colorectal cancer, Br. J. Surg. 93 (2006) 395–406.
[33] S.A. Kuismanen, M.T. Holmberg, R. Salovaara, A. de la Chapelle, P. Peltomaki, Genetic and epigenetic modification of MLH1 accounts for a major share of microsatellite-unstable colorectal cancers, Am. J. Pathol. 156 (2000) 1773–1779.
[34] G. Deng, A. Chen, J. Hong, H.S. Chae, Y.S. Kim, Methylation of CpG in a small region of the hMLH1 promoter invariably correlates with the absence of gene expression, Cancer Res. 59 (1999) 2029–2033.
[35] Y. Miyakura, K. Sugano, F. Konishi, A. Ichikawa, M. Maekawa, K. Shitoh, S. Igarashi, K. Kotake, Y. Koyama, H. Nagai, Extensive methylation of hMLH1 promoter region predominates in proximal colon cancer with microsatellite instability, Gastroenterology 121 (2001) 1300–1309.
[36] T. Furukawa, F. Konishi, S. Masubuchi, K. Shitoh, H. Nagai, T. Tsukamoto, Densely methylated MLH1 promoter correlates with decreased mRNA expression in sporadic colorectal cancers, Genes Chromosomes Cancer 35 (2002) 1–10.
[37] Z. Xiong, P.W. Laird, COBRA: a sensitive and quantitative DNA methylation assay, Nucleic Acids Res. 25 (1997) 2532–2534.
[38] N.J. Hawkins, R.L. Ward, Sporadic colorectal cancers with microsatellite instability and their possible origin in hyperplastic polyps and serrated adenomas, J. Natl. Cancer Inst. 93 (2001) 1307–1313.
[39] M.J. O'Brien, S. Yang, C. Mack, H. Xu, C.S. Huang, E. Mulcahy, M. Amorosino, F.A. Farraye, Comparison of microsatellite instability, CpG island methylation phenotype, BRAF and KRAS status in serrated polyps and traditional adenomas indicates separate pathways to distinct colorectal carcinoma end points, Am. J. Surg. Pathol. 30 (2006) 1491–1501.
[40] J.R. Jass, Classification of colorectal cancer based on correlation of clinical, morphological and molecular features, Histopathology 50 (2007) 113–130.
[41] K. Hamatani, H. Eguchi, K. Takahashi, K. Koyama, M. Mukai, R. Ito, M. Taga, W. Yasui, K. Nakachi, Improved RT-PCR amplification for molecular analyses with long-term preserved formalin-fixed, paraffin-embedded tissue specimens, J. Histochem. Cytochem. 54 (2006) 773–780.

Reprint Sales Europe & ROW
Deirdre Dunne

Tel: +31 (0)20 485 3440
Fax: +31 (0)20 485 3280

D.dunne@elsevier.com

Reprint Sales North America
Nicholas Pavlow

Tel: +1 212 633 3960
Fax: +1 212 462 1915

N.pavlow@elsevier.com

INFECTION AND IMMUNITY, Oct. 2008, p. 4783–4791 Vol. 76, No. 10
0019-9567/08/$08.00+0 doi:10.1128/IAI.01612-07

Cytolethal Distending Toxin Induces Caspase-Dependent and -Independent Cell Death in MOLT-4 Cells[▽]

Masaru Ohara,[1]* Tomonori Hayashi,[2] Yoichiro Kusunoki,[2] Kei Nakachi,[2] Tamaki Fujiwara,[1] Hitoshi Komatsuzawa,[1] and Motoyuki Sugai[1]

Department of Bacteriology, Hiroshima University Graduate School of Biomedical Sciences, Kasumi 1-2-3, Minami-ku, Hiroshima, Hiroshima 734-8553, Japan,[1] and Department of Radiobiology and Molecular Epidemiology, Radiation Effects Research Foundation, 5-2 Hijiyama Park, Minami-ku, Hiroshima, Hiroshima 732-0815, Japan[2]

Received 6 December 2007/Returned for modification 28 April 2008/Accepted 7 July 2008

Cytolethal distending toxin (CDT) induces apoptosis using the caspase-dependent classical pathway in the majority of human leukemic T cells (MOLT-4). However, we found the process to cell death is only partially inhibited by pretreatment of the cells with a general caspase inhibitor, z-VAD-fmk. Flow cytometric analysis using annexin V and propidium iodide showed that a 48-h CDT treatment decreased the living cell population by 35% even in the presence of z-VAD-fmk. z-VAD-fmk completely inhibited caspase activity in 24 h CDT-intoxicated cells. Further, CDT with z-VAD-fmk treatment clearly increased the cell population that had a low level of intracellular reactive oxygen. This is a characteristic opposite to that of caspase-dependent apoptosis. Overexpression of *bcl2* almost completely inhibited cell death using CDT treatment in the presence of z-VAD-fmk. The data suggest there are at least two different pathways used in CDT-induced cell death: conventional caspase-dependent (early) apoptotic cell death and caspase-independent (late) death. Both occur via the mitochondrial membrane disruption pathway.

Programmed cell death is critical for organ development and homeostasis in eukaryotes (24, 49, 52). In the past, the caspases were considered essential proteases for apoptosis. However, accumulating data suggest that caspase-independent cell death occurs in programmed cell death (4, 23) and, in certain conditions, the caspase-independent pathway is an important mechanism to protect organs when caspase-dependent cell death does not occur (4).

Viral or bacterial infection and cancer often influence programmed cell death pathways. This is true of death induced by the cytolethal distending toxin (CDT), one of the bacterial toxins produced by *Aggregatibacter actinomycetemcomitans*, a gram-negative pathogen implicated in the pathogenesis of juvenile and adult periodontitis (39, 42). CDT was demonstrated to induce apoptosis in various cell types, including the T-lymphocytic leukemia cell lines, Jurkat cells, and MOLT-4 cells (31, 35, 50).

CDT belongs to a family of toxins with cell cycle specific inhibitory activity blocking the G_2 to M phase through inactivation of the CDC2/cyclin B complex (for recent reviews, see references 17, 30, and 32). CDT is a complex of three subunits: CdtA, CdtB, and CdtC. CdtB induces double-strand breaks, acting as a DNase that triggers the CDT intoxication (9, 25). CdtA and CdtC have homologies to lectin-like domains that can bind to surface molecules on the target cells (7). CDT internalizes through a receptor-mediated endocytosis and subsequently reaches the nucleus by retrograde transport and active nuclear pore transport (15, 29). In the nucleus, the CDT-induced chromatin injury is found as double-strand breaks that may recruit a large protein complex, the PIDDosome, in which caspase-2 activation occurs (44). Previously, we demonstrated that CDT induces apoptosis and activates caspase-2 in two T-cell leukemia cell lines, Jurkat and MOLT-4 (31). Activated caspase-2 acts as an upstream initiator of mitochondrial membrane permeability (22). Increased permeability of the mitochondrial membrane releases proapoptotic molecules, including cytochrome *c*, to activate executive caspases, and this loss of the mitochondrial membrane potential leads to the production of reactive oxygen species (ROS) (34). In the presence of a caspase inhibitor, CDT-induced apoptosis was completely blocked for 16 h in Jurkat cells, suggesting that CDT-induced cell death was dependent on caspase activation (31). However, we found that some of the cells, after 24 h of CDT intoxication, undergo death in a manner different from conventional apoptosis using caspase activation. Here, we report the detailed features of this cell death and discuss the importance of caspase-independent cell death during late-stage CDT-intoxication.

MATERIALS AND METHODS

Purification of *A. actinomycetemcomitans* CDT. CDT holotoxin was purified by using a Ni-chelated agarose resin column as described previously where the C-terminal His_6-tagged CdtC was expressed using the pQE 60 expression vector in M15 *Escherichia coli* (Qiagen, Tokyo, Japan) that carried the *A. actinomycetemcomitans cdtA*, *cdtB*, and *cdtC* genes downstream of the T5 promoter (31). A mutant CDT with CdtB His274Ala (*cdtB* 274 histidine changed to alanine) was purified by using the same method. The mutant was constructed by using site-directed mutagenesis of the 274th histidine residue to an alanine in the *cdtB* gene of pQEcdtABC and was performed by using the overlap extension method (46). The primers used were 5′-ACA TCC GAT gcT TTT CCT GTT-3′ and 5′-AAC AGG AAA Agc ATC GGA TGT-3′ (mutated sites are shown as lowercase letters). The mutant DNA containing *cdtAB(H274A)C* was subcloned into the pQE60 vector (Qiagen).

* Corresponding author. Mailing address: Department of Bacteriology, Hiroshima University Graduate School of Biomedical Sciences, Kasumi 1-2-3, Minami-ku, Hiroshima, Hiroshima 734-8553, Japan. Phone: (81) 82 257 5636. Fax: (81) 82 257 5639. E-mail: mohara@hiroshima-u.ac.jp.

▽ Published ahead of print on 21 July 2008.

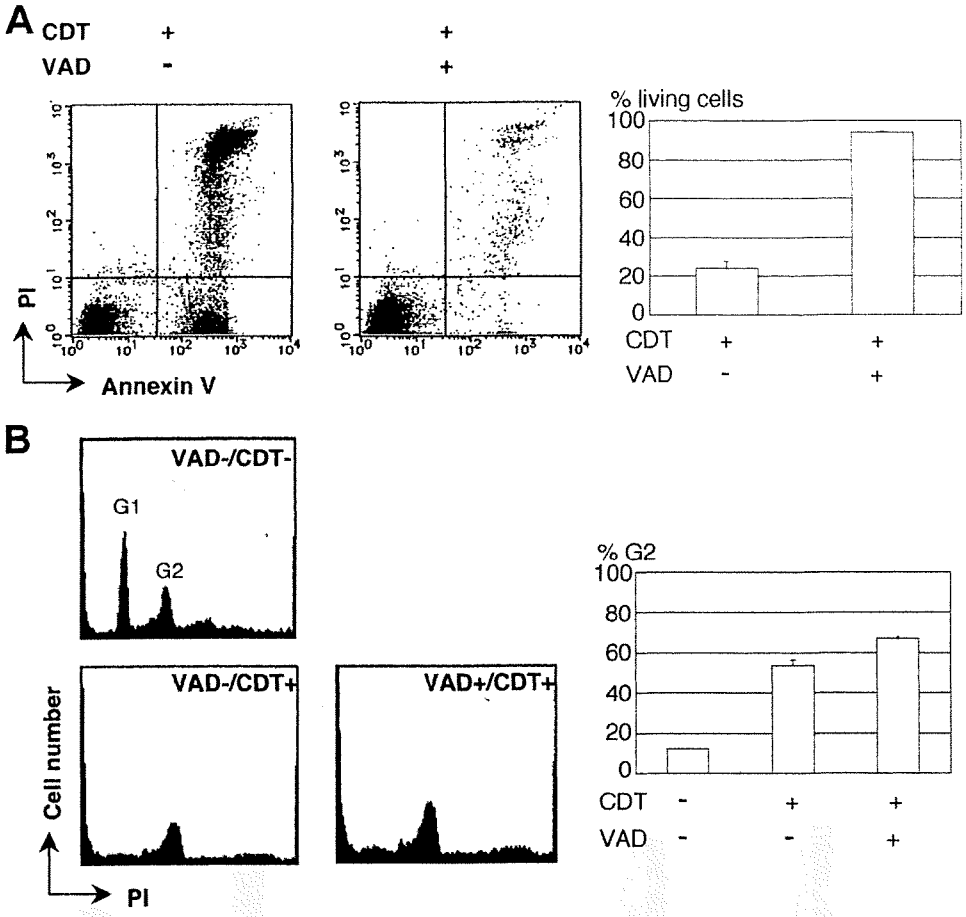

FIG. 1. Early effects of CDT intoxication on MOLT-4 cells in the presence of the general caspase inhibitor, z-VAD-fmk. The effects of CDT on MOLT-4 cells were examined 16 h after pretreatment of the cells with or without the general caspase inhibitor, z-VAD-fmk (100 μM), for 30 min. (A) MOLT-4 cells treated with CDT (100 ng/ml) for 16 h were observed after staining with PI and FITC-labeled annexin V for fluorescence by using a FACSCalibur. The percentages of living (annexin V-negative, PI-negative) cells are shown in the graphs along with the standard deviations. (B) The cell cycle was determined by staining the cells with PI after fixing the cells with 70% ethanol and RNase treatment. The percentages of the cells in the G_2 phase are shown in the graph, along with the standard deviations.

Preparation of cells and culture conditions. The thymic T-cell leukemia cell line, MOLT-4, and the peripheral T-cell leukemia cell line, Jurkat, were cultured in RPMI 1640 with 10% fetal calf serum (FCS), 100 U of penicillin G/ml, and 100 μg of streptomycin/ml and incubated at 37°C using 5% CO_2 incubator. Cells (10^6 cells/ml) were treated with or without CDT (100 ng/ml) and cultured under similar conditions. In some experiment, cells were X-irradiated. Irradiation of cells was performed by an X-ray generator (Shimadzu HF-320; 220 kVp, 8 mA) with a 0.5-mm aluminum and 0.3-mm copper filter at a dose of ~0.8 Gy/min. Cells were irradiated in a plastic dish at room temperature. z-VAD-fmk, a general caspase inhibitor (MBL Nagoya, Japan), was used at 100 μM and was added 30 min before CDT treatment.

Establishing MOLT-4 cells stably overexpressing *bcl-2*. The complete coding sequence of *bcl-2* (19), the gene governing antiapoptotic mitochondrial outer membrane permeabilization (MOMP), was amplified by using the PCR and subsequently cloned into an SFFV-neo vector (14). MOLT-4 cells were stably transfected with the plasmid SFFV-human *bcl-2* or a control plasmid, SFFV-neo, using electroporation at 350 V with a capacitance of 960 μF with a GenePulser (Bio-Rad, Richmond, CA). Transfected cells were selected in medium containing 0.5 mg of G418/ml for 30 days. *bcl-2* transfectants were found by using fluorescence-activated cell sorting (FACS) and Western analysis with Bcl-2 monoclonal antibody, 6C8 (BD Pharmingen, San Jose, CA), where we demonstrated Bcl-2 levels increased 10- to 20-fold greater than Bcl-2 present in untransfected or SFFV-neo-transfected MOLT-4 cells. The cells stably expressing Bcl-2 are referred to as MOLT-4bcl2 cells. The cells transfected with the control plasmid SFFV-neo served as a control and are referred to as MOLT-4neo cells.

Flow cytometry. Conformational change in the membrane by phosphatidylserine translocation and membrane hole formation was observed by counting the cell population stained with fluorescein isothiocyanate (FITC)-labeled annexin V and propidium iodide (PI) as described previously (31). Briefly, CDT-treated cells (5×10^5 to 10×10^5) were centrifuged at $350 \times g$ for 2 min and washed three times with 500 μl of phosphate-buffered saline (PBS; 137 mM NaCl, 2.7 mM KCl, 8.1 mM Na_2HPO_4, 1.5 mM KH_2PO_4 [pH 7.3]) with 1% FCS. The washed cells were resuspended in 180 μl of PBS containing 1% FCS, 0.5 μl of FITC-labeled annexin V, and 1 μl of PI using a MEBCYTO apoptosis kit (MBL, Nagoya, Japan). After 5 min at room temperature, 10,000 cells were scanned by using a FACScan (BD Biosciences, San Jose, CA). We performed a quadrant population analysis using CellQuest software (BD Biosciences). The live cell population was negative for both annexin V and PI (shown in the lower left quadrant).

Hydroethidine (HE) was used to measure the intracellular ROS, the superoxide anion ($O_2 \cdot^-$) (16). HE (5 mM) was added to the PBS-washed cells (5×10^5 cells in 500 μl of PBS with 1% FCS). Cells were incubated for 20 min at 37°C. After a wash with PBS using centrifugation at $350 \times g$ for 5 min, the cells were resuspended in 200 μl of PBS containing 1% FCS and scanned using the FACScan. A gated population analysis was performed by using CellQuest software (BD Biosciences).

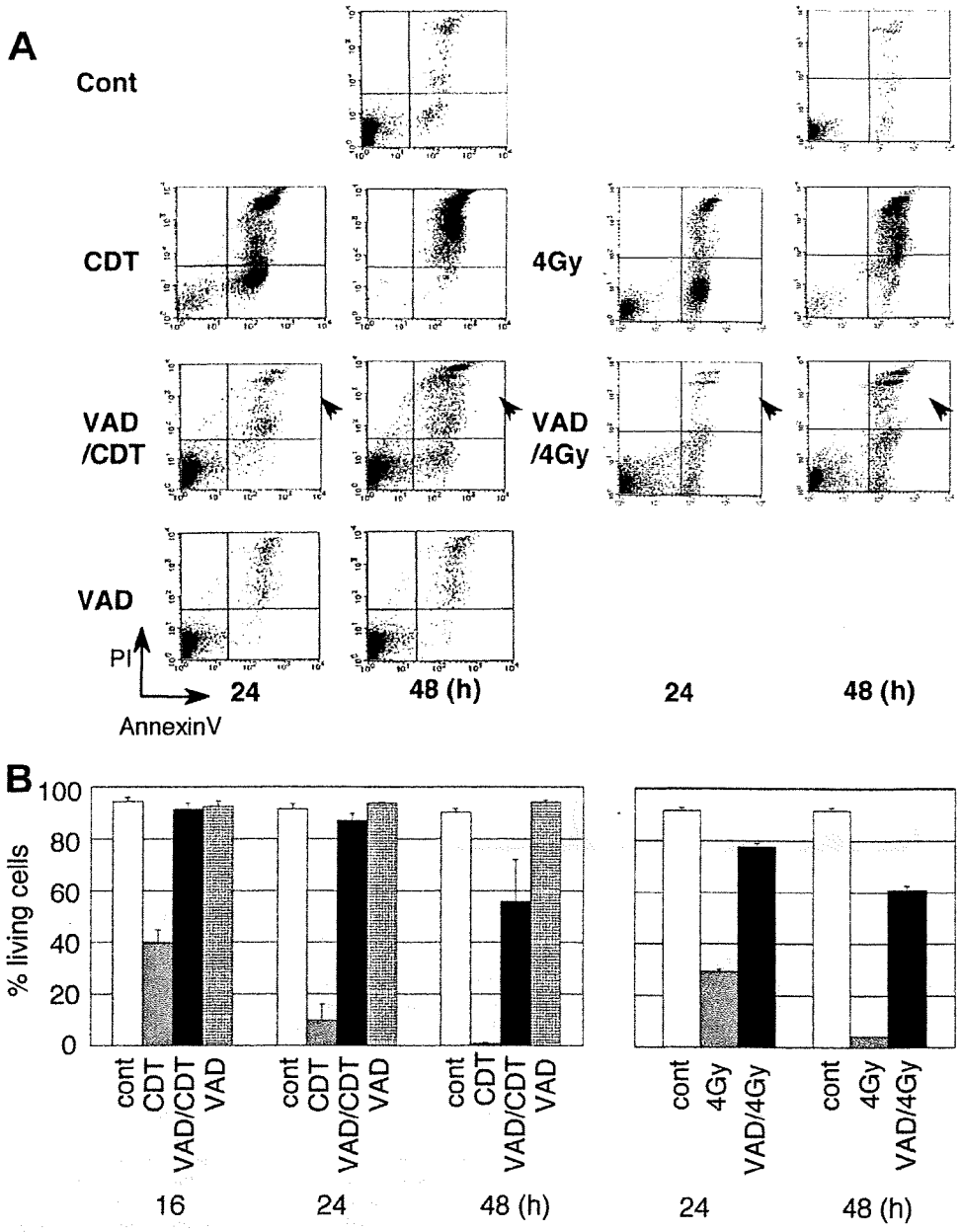

FIG. 2. Late effects of CDT in MOLT-4 cells in the presence of z-VAD-fmk. CDT-induced cell death was monitored in MOLT-4 cells at 24 h or 48 h after CDT treatment (100 ng/ml) in the presence or absence of z-VAD-fmk (100 μM). (A) Cell death was observed by using a FACScan after staining with PI and FITC-labeled annexin V. (B) Percentages of living (annexin V-negative, PI-negative) cells at 16, 24, and 48 h. As a control, radiation-induced cell death was monitored in MOLT-4 cells at 24 and 48 h with or without z-VAD-fmk. Arrowheads show that dead cell populations increased at 48 h even in the presence of z-VAD-fmk after treatment with CDT or radiation.

The cell cycle was determined as follows. CDT-treated cells were washed twice with PBS and fixed with 70% ethanol for 2 h at 4°C. The fixed cells were washed twice with PBS and incubated with 0.25 mg of RNase A/ml for 15 to 60 min at 37°C. DNA in the RNase-digested cells was stained with 50 μg of PI/ml for 30 min at 4°C and analyzed by using a FACSCalibur flow cytometer (BD Biosciences).

Caspase assay. CDT-treated cells were harvested and washed with PBS. PBS-washed cells were lysed with lysis buffer (10 mM Tris-Cl [pH 7.4], 25 mM NaCl, 0.25% Triton X-100, 1 mM EDTA) and centrifuged at 15,000 × *g* for 10 min. The supernatant was diluted with lysis buffer at a protein concentration adjusted to 1 mg/ml. Then, 5 μg of total protein was incubated with 200 μl of caspase buffer (50 mM Tris-Cl [pH 7.2], 100 mM NaCl, 1 mM EDTA, 10% sucrose, 0.1% CHAPS {3-[(3-cholamidopropyl)-dimethylammonio]-1-propanesulfonate}, 5 mM dithiothreitol) using 50 μM concentrations of the various fluorigenic substrate peptides. The peptides used were Ac-DEVD-7-amino-4-methyl cumarine (AMC) for caspase-3, caspase-7, and caspase-8; Ac-IETD-AMC for caspase-8, caspase-6, and Granzyme; Ac-LEHD-AMC for caspase-9; and Ac-VDVAD-AMC for caspase-2 (Peptide Institute, Inc., Osaka, Japan). The reaction mixture

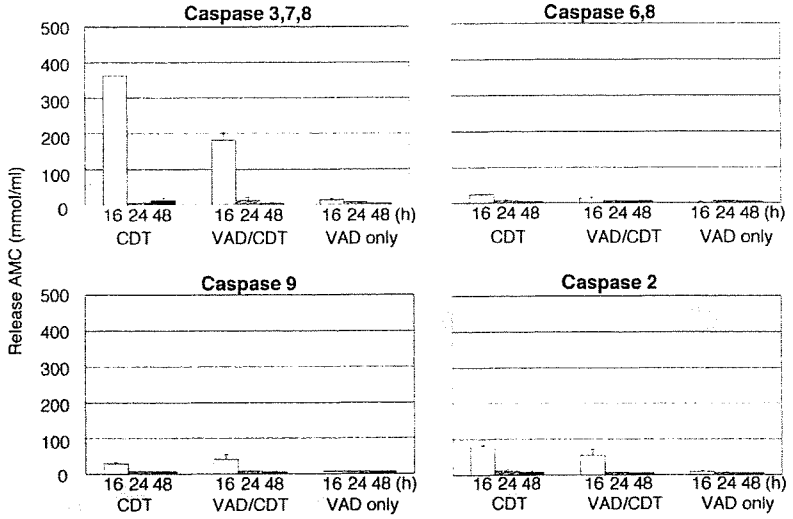

FIG. 3. Caspase activities in CDT-treated MOLT-4 cells in the presence of z-VAD-fmk. Caspase activities were monitored in MOLT-4 cells at 24 or 48 h after CDT treatment (100 ng/ml) in the presence or absence of z-VAD-fmk (100 μM). CDT-treated cell extracts (5 μg of total protein) were incubated with 50 μM concentrations of the various fluorigenic substrate peptides: AMC for caspase-3, caspase-7, and caspase-8; Ac-DQTD-AMC for caspase-7 and caspase-3; Ac-IETD-AMC for caspase-8, caspase-6, and Granzyme; Ac-LEHD-AMC for caspase-9; and Ac-VDVAD-AMC for caspase-2 (Peptide Institute, Inc., Osaka, Japan). The reaction mixture was incubated at 37°C for 60 min, where the release of AMC was measured by using a fluorometer (Shimazu RF-540) with an excitation at 380 nm and an emission at 460 nm.

was incubated at 37°C for 60 min where the release of 7-amino-4-methylcumarin was measured by using a fluorometer (Shimazu RF-540) with an excitation at 380 nm and an emission at 460 nm.

RESULTS

Early effect of CDT in MOLT-4 cells in the presence of the general caspase inhibitor, z-VAD-fmk. The effect of the general caspase inhibitor, z-VAD-fmk, on MOLT-4 cells was examined for 16 h after the cells were treated with 100 ng of CDT/ml. As shown in Fig. 1, when the cells were treated with z-VAD-fmk (100 μM) most cells retained the phenotype of living cells (annexin V negative, PI negative). This indicated the caspase inhibitor almost completely blocked CDT-induced apoptosis for at least 16 h but did not block the G_2/M arrest (Fig. 1B). We investigated DNA ladder formation in the presence of z-VAD-fmk in the CDT-treated MOLT-4 cells. z-VAD-fmk completely inhibited internucleosomal DNA fragmentation (data not shown). These results are consistent with our previous study using Jurkat cells (31).

Late effect of CDT in MOLT-4 cells in the presence or absence of z-VAD-fmk. We then assessed the effect of long-term exposure to CDT on MOLT-4 cells in the presence or absence of z-VAD-fmk. A 24-h exposure to CDT on MOLT-4 cells increased the population of annexin V-positive and PI-negative cells, as well as a population of annexin V-positive and PI-positive (dead) cells (Fig. 2A). Pretreatment with z-VAD-fmk significantly inhibited the increase of these populations at 24 h (Fig. 2A). At 48 h, however, a population of annexin V-positive and PI-negative cells and also a population of annexin V-positive and PI-positive cells increased compared to the numbers at 16 h (Fig. 1 and 2). At 48 h after CDT exposure in the presence of z-VAD-fmk, living cells defined as annexin V-negative and PI-negative cells decreased by 35% compared to nontreated cells (90.18% living) (Fig. 2B). This is very similar to the observation when MOLT-4 cells were X-irradiated (5). Ionizing radiation on MOLT-4 cells induced G_2/M arrest (37). Moreover, pretreatment of z-VAD-fmk inhibited the increase of dead cells at 24 h (Fig. 2A) (5). However, at 48 h after X-irradiation in the presence of z-VAD-fmk, the number of living cells decreased. With CDT treatment, caspase activities increased after 16 h (Fig. 3). This was apparent for caspase-3, caspase-7, and caspase-8. However, pretreatment with z-VAD-fmk significantly suppressed caspase activity, and this was likewise observed in Jurkat cells (31). Further, there was almost no caspase activity in MOLT-4 cells at 24 h after CDT exposure in the presence of z-VAD-fmk, even though 85% of the cells were alive (Fig. 2B and 3). This was also found at 48 h after CDT exposure in the presence of z-VAD-fmk. This suggests that CDT is able to induce cell death in the late stages of cell intoxication without caspase activation.

Comparison of the late effects of CDT to the mutant CdtB His274Ala CDT. Previous studies suggest CdtB shows sequence similarity to DNase I, where it shares conserved amino acids essential for Mg binding (9, 25). The 274th histidine residue in the CdtB subunit is one of the active sites where a mutation at 274th His to Ala abolishes CDT cytodistending and cell cycle arrest activities (28). This strongly suggests that CdtB acts as a nuclease. To determine whether the CdtB nuclease activity is responsible for CDT-induced late cell death, mutant CDT containing CdtB H274A was generated and added to the medium of MOLT-4 cells. Mutated CDT did not show cytokilling activity until 24 h, as expected (Fig. 4). By 48 h, ca. 20% of the cells treated with the mutant CDT were dead, and this late cell death was almost completely inhibited by pretreatment with z-VAD-fmk. This shows that the possible nuclease activity of CdtB is also important for late cell

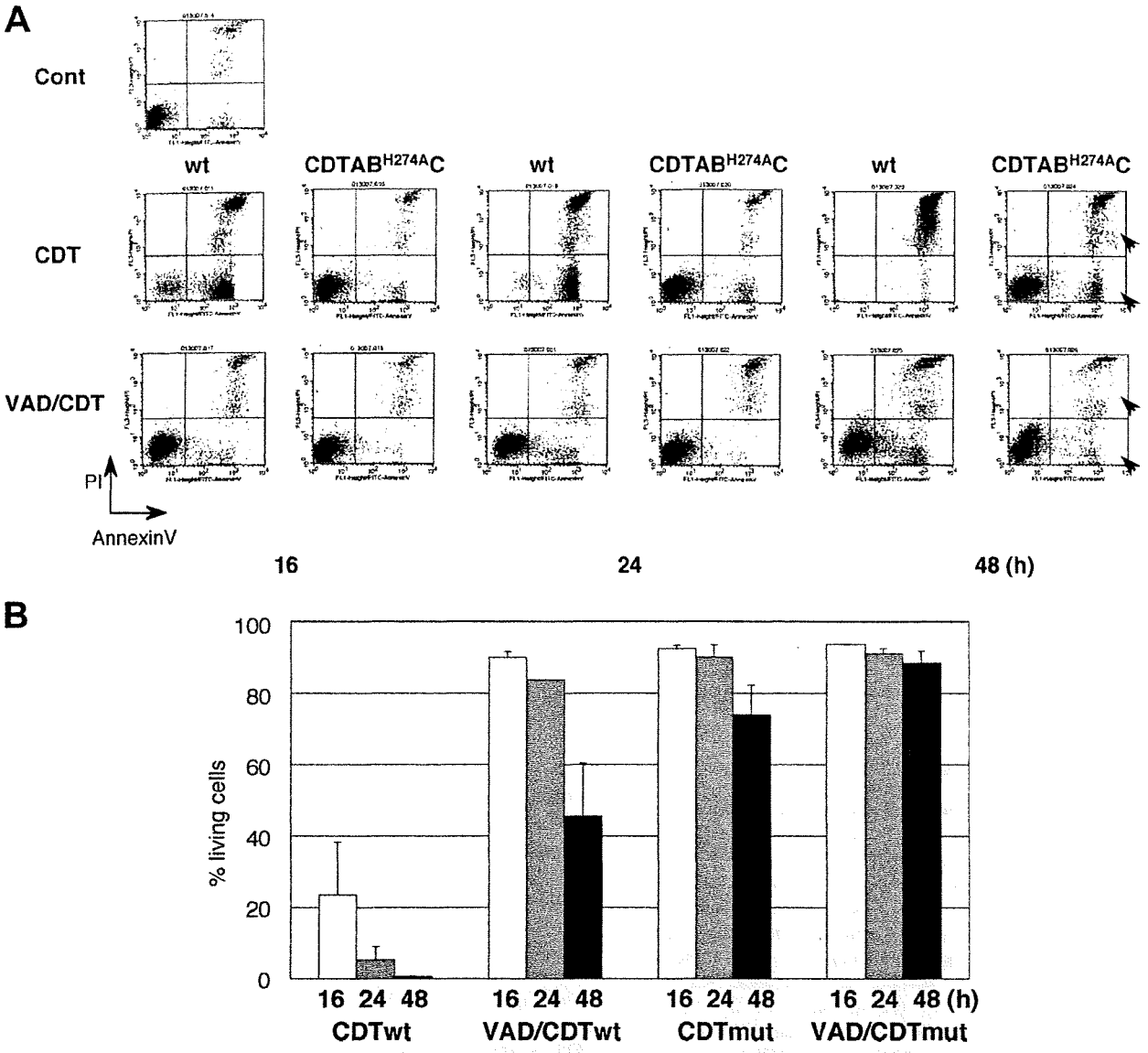

FIG. 4. Effects of mutated CDT on MOLT-4 cells in the presence or absence of z-VAD-fmk. CDT-induced cell death was monitored at 24 or 48 h in MOLT-4 cells after CDT treatment (100 ng/ml) or mutated CdtB His274Ala CDT. (A) Cell death was analyzed by using a FACScan after staining with PI and FITC-labeled annexin V. (B) Percentages of living (annexin V-negative, PI-negative) cells at16, 24, and 48 h. Arrowheads show that dead cell populations increased at 48 h after treatment with CDT but was not seen in the presence of z-VAD-fmk.

death and was not inhibited by the general caspase inhibitor, z-VAD-fmk.

CDT-induced cell death in MOLT-4 cells overexpressing the *bcl2* gene. We previously demonstrated that CDT induces mitochondrial membrane permeability, resulting in an apoptotic cell death (early cell death) (31). To determine the role of mitochondria in late-stage CDT-induced cell death, we examined MOLT-4 cells forced to overexpress the *bcl2* gene (MOLT-4/bcl2). As shown in Fig. 5A, Bcl2 overexpression showed an inhibitory effect on the increase of the population of annexin V-positive, PI-positive cells using CDT intoxication. After 48 h of CDT intoxication, a 23% decrease in the living cell population was observed in CDT-treated MOLT-4/bcl2 cells (72% alive) compared to nontreated cells (95% alive) (Fig. 5B). This shows that CDT-induced cell death was significantly attenuated by the overexpression of *bcl2* in MOLT-4 cells. Further, pretreatment of MOLT-4/bcl2 with z-VAD-fmk completely inhibited CDT-induced cell death for 48 h (Fig. 5A [arrowheads] and B). This finding suggests that increased permeability of the mitochondrial membrane is a central factor in the overall cell death by CDT intoxication.

Appearance of a cell fraction with a low level of superoxide anion in CDT-treated MOLT-4 in the presence of z-VAD-fmk. Caspase-dependent apoptosis is characterized by an increase

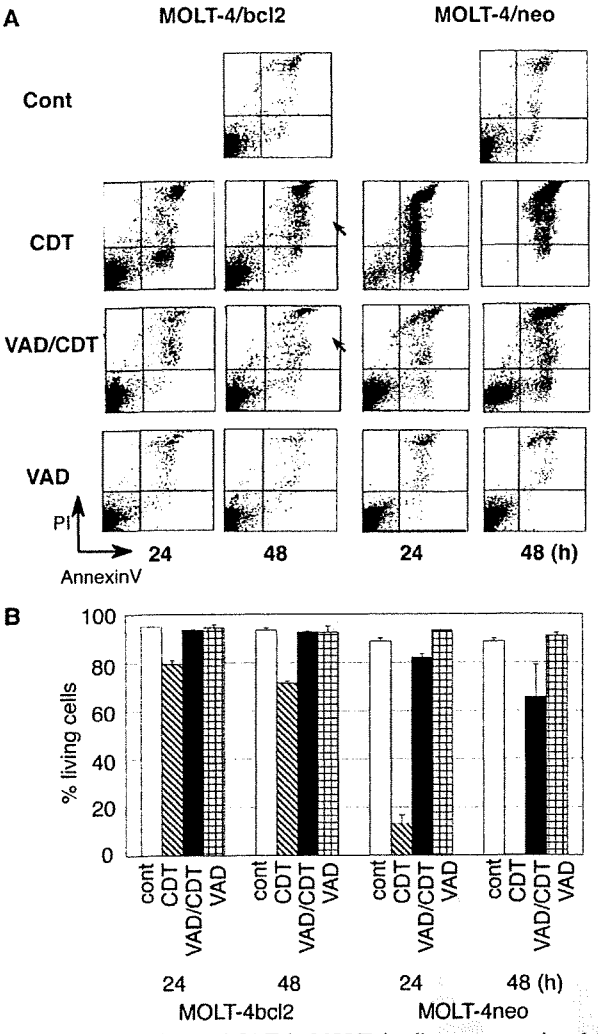

FIG. 5. Late effects of CDT in MOLT-4 cells overexpressing the *bcl2* gene in the presence or absence of z-VAD-fmk. CDT-induced cell death was monitored at 24 or 48 h after the treatment in MOLT-4 cells that were forced to overexpress the *bcl2* gene (MOLT-4/bcl2), MOLT-4 cells transfected with pSFFV-neo vector only (MOLT-4/neo), and parental MOLT-4 cells. (A) Cell death was analyzed by using a FACScan after staining with PI and FITC-labeled annexin V. (B) Percentages of living (annexin V-negative, PI-negative) cells at 48 h. Arrowheads show that dead cell populations increased at 48 h after treatment with CDT but was not seen in the presence of z-VAD-fmk.

in the intracellular superoxide anion and is related to mitochondrial membrane activity. We examined the levels of superoxide anion in CDT-treated cells using HE that reacts with superoxide anion. Concomitantly, FITC-labeled annexin V and PI were used to detect apoptotic and dead cell populations, respectively. We divided the cell population obtained by FACS into four groups (Fig. 6A): (i) S1 with normal levels of superoxide anion and nonapoptotic annexin V-negative, (ii) S2 with low levels of superoxide anion and annexin V negative, (iii) S3 with high level levels of superoxide anion and apoptotic annexin V positive, and (iv) S4 with low levels of superoxide anion (low HE) or at a normal level and apoptotic annexin V positive. Compensation between HE and PI was adjusted to separate the locations for the PI-positive and PI-negative (dead/live) populations in the quadrant analysis, where the PI-positive population is shown as dark red. As shown in Fig. 6, CDT treatment increased the S3 population to a maximum at 16 h, together with the appearance of a PI-positive dead cell population. Longer exposure increased the PI-positive population, as well as the S4 population. This shows that the CDT-induced early apoptosis was followed by cell death. We then assessed the population change in MOLT-4 cells exposed to CDT in the presence of z-VAD-fmk. z-VAD-fmk induced the appearance of an S2 population in CDT-treated MOLT-4 cells at 16 h, at which point the S3 population did not increase. At 48 h, the cells in the S2 population decreased and PI-positive population, as well as the S4 population, increased. MOLT-4/bcl2 cells exposed to CDT in the presence of z-VAD-fmk showed most cells remained in the S1 population even after 48 h of intoxication (data not shown). This, together with the caspase assay, clearly shows that CDT intoxication in the presence of z-VAD-fmk induced MOLT-4 cells into a caspase-independent nonapoptotic cell death, where MOMP played a significant role.

DISCUSSION

We show here that long exposure to CDT killed MOLT-4 cells even if caspase activation was inhibited by z-VAD-fmk. A similar observation was reported when MOLT-4 cells were X-irradiated in the presence of z-VAD-fmk (5). X-irradiation induces caspase-3-dependent apoptosis, but treatment of inhibitor of caspase-3 was not accompanied by any persistent increase in cell survival. Instead, irradiated cells treated by the inhibitor exhibited characteristics of a necrotic cell death. Similarly, our results show that caspase-dependent and caspase-independent pathways are involved in the CDT-induced MOLT-4 cell deaths. Similar responses of CDT-intoxicated MOLT-4 cells and X-irradiated MOLT-4 cells further support the idea that CDT intoxication triggers DNA damage.

Preincubation with z-VAD-fmk almost completely inhibited CDT-induced cell death in MOLT-4 cells overexpressing *bcl2* that increases the stability of the mitochondrial membrane. The data shows CDT-induced cell death is mitochondrion dependent and suggests the caspase-dependent and caspase-independent death pathways converge at the mitochondria (45). Reports demonstrate death signaling through the mitochondrial pathways induces MOMP to release several mitochondrial proteins including cytochrome *c* (13, 47, 48), where the Bcl-2 family of proteins are considered to be important regulatory factors for MOMP (8, 41). A possible reason why general caspase inhibitors fail to prevent cell death is because these inhibitors lack the ability to inhibit MOMP (8, 10, 21).

CDT is not the only bacterial toxin that induces cell death through multiple pathways. *Staphylococcus aureus* alpha-toxin, the major hemolysin, induces massive cell necrosis by forming pores in lipid bilayers at high doses (>6 μg/ml). At low doses, this toxin can induce DNA fragmentation and caspase activation, the typical classical apoptosis pathway, and also caspase-independent cell death (11). *Streptococcus pneumoniae* induces a rapid caspase-independent cell death in cultured bone mar-

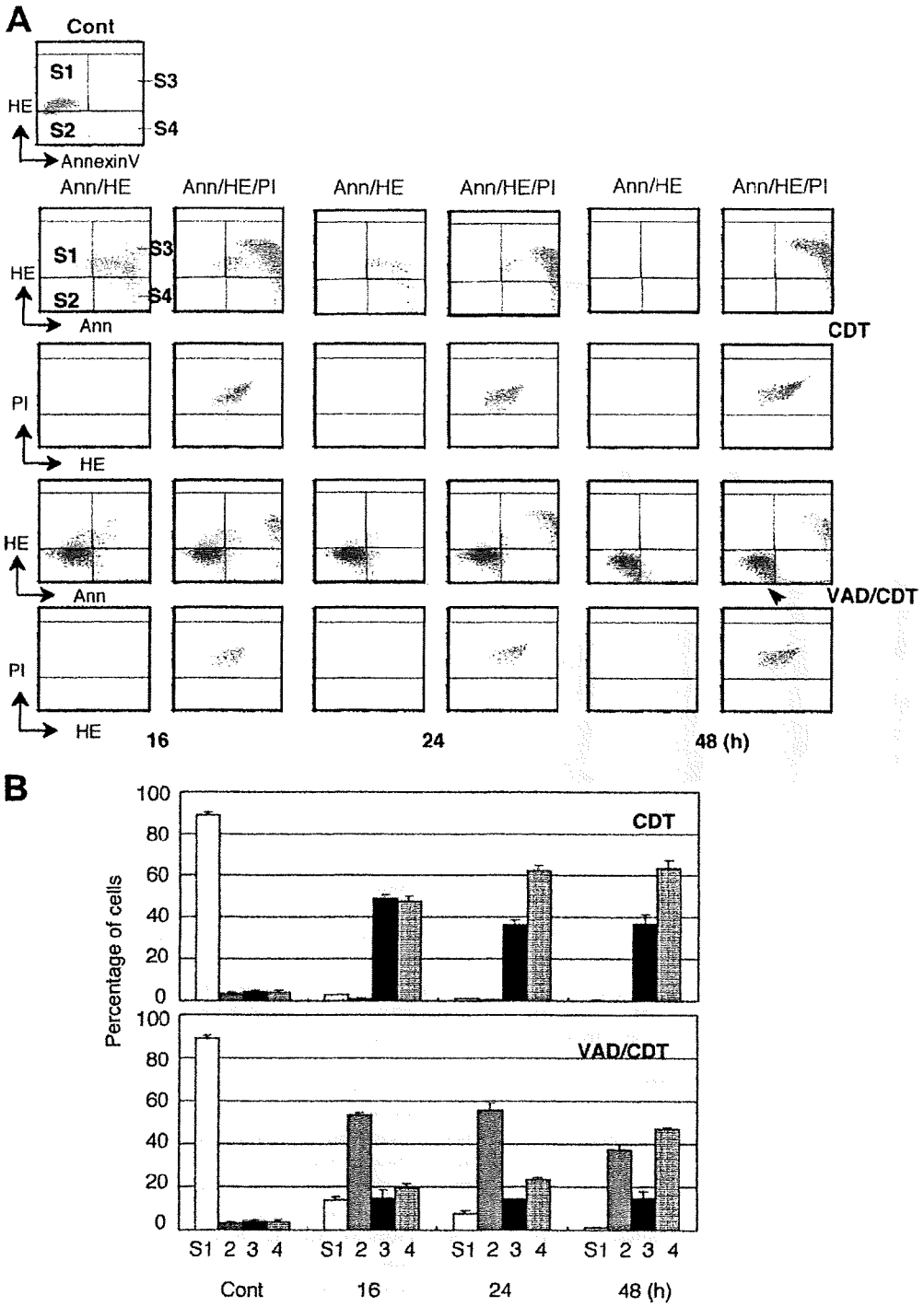

FIG. 6. ROS and phosphatidylserine translocation in CDT-treated MOLT-4 cells in the presence or absence of z-VAD-fmk. (A) The levels of ROS and phosphatidylserine translocation in the cytoplasmic membrane in the CDT-treated MOLT-4 cells were measured at 24 and 48 h by using a FACScan. To monitor the dead cells, the cells were subjected to double (Ann/HE) and triple (Ann/HE/PI) staining. Compensation between HE and PI was adjusted to separate the locations of PI-positive and PI-negative populations in the quadrant analysis. PI-positive populations were gated and are shown in the quadrant analysis of HE and annexin V double staining as a dark red color. S1, region of cells with normal levels of HE and annexinV; S2, cells with low levels of HE; S3, cells with high levels of HE and annexin V binding; S4, cells with low levels of HE and high levels of annexin V binding. The arrowhead shows an increased population in S2 by pretreatment with z-VAD-fmk, i.e., cells with a low level of ROS. (B) Percentages of cells distributed into the fractions at 16, 24, and 48 h, where CDT indicates the cells treated with 100 ng of CDT alone/ml and VAD/CDT indicates CDT-treated cells after pretreatment with z-VAD-fmk (100 μM).

row-derived dendritic cells (6). This induction is dependent on the expression of pneumolysin, one of the major cytotoxins of *S. pneumoniae*. This is followed by the delayed onset of caspase-dependent cell death associated with the terminal maturation of dendritic cells. *Escherichia coli* heat-labile enterotoxin is composed of a single catalytically active A subunit and a pentameric B subunit that interacts with a receptor that mediates the uptake of the holotoxin into the target cells (38). Interestingly, the nontoxic B subunit induces both caspase-dependent and -independent cell death in CD8 T cells. The enterotoxin B subunit induces a rapid loss of mitochondrial membrane potential where cell viability is not affected by caspase inhibitors, suggesting some other intracellular signaling pathways are involved following interaction with the B subunit receptor. Another example is *Clostridium difficile* toxin B (33). *C. difficile* toxin B inactivates small GTPases, Rho, Rac, and Cdc42, which lead to caspase-3 activation in HeLa cells. Caspase inhibitors delayed cell death but did not alter the consequence.

Several classifications are proposed to differentiate types of cell death (1, 4, 12, 23). For example, Kroemer et al. (23) proposes four types: (i) classical apoptosis showing programmed cell death through caspase activation; (ii) apoptosis-like cell death resembling apoptosis but lacking total chromatin condensation, karyorhexis, and oligonucleosomal DNA fragmentation (20, 43); (iii) autophagic cell death with an accompanying accumulation of autophagic vacuoles in the cells (36, 51); and (iv) necrosis exhibiting pronounced swelling of the cytoplasmic organelles (18, 48).

Caspases, a group of cysteine proteases, normally act only during classical apoptosis; however, the activation of caspases is also observed in apoptosis-like autophagic cell death, and necrosis as well (36, 43, 48, 51). Further, caspases may be activated not only during the lethal process but also in nonlethal signal transduction (27). Paradoxically, accumulating evidence suggests several types of programmed cell deaths occur without caspase activation in parallel to caspase-dependent cell death as found in apoptosis-like cell death, autophagic cell death, and necrosis (2, 3, 13, 40). Fink et al. (12) propose four types of dying cells caused by infection with microorganisms: apoptosis, autophagy, oncosis, and pyroptosis. Apoptosis is a form of caspase-mediated cell death with particular morphological features, e.g., the apoptotic body, without inflammation. Oncosis is a prelethal process that occurs in ATP-depleted cells concomitant with morphological swelling and eventual membrane permeability. Autophagic cell death involves degradation of intracellular components using autophagic vacuoles. Pyroptosis is a pathway to cell death that involves interleukin-1-mediated inflammation.

Although several morphotypes have been proposed, a definitive classification of the types of cell death pathways has not been established. This is probably because there may be some signaling pathways overlapping and sharing the different death programs (4, 26). It has also been proposed that a dominant cell death morphotype may be determined by comparing the rapidity of the available death programs, i.e., the fastest and most effective pathway among them is dominant (4). In the case of CDT intoxication, the caspase-2-related classical pathway may be the fastest and most efficient pathway. Identification of molecule(s) involved in the CDT-induced caspase-independent and the MOMP-dependent pathway is required to further characterize this death pathway.

ACKNOWLEDGMENTS

We thank the Research Facilities of the Hiroshima University School of Dentistry and School of Medicine for the use of their facilities. We are grateful to Jim Nelson for editorial assistance.

This study was supported in part by a grant for development of highly advanced medical technology (type A) and a grant-in-aid for research (type C) from the Ministry of Education, Science, Sports, and Culture of Japan.

REFERENCES

1. **Abraham, M. C., and S. Shaham.** 2004. Death without caspases, caspases without death. Trends Cell Biol. **14**:184–193.
2. **Borner, C., and L. Monney.** 1999. Apoptosis without caspases: an inefficient molecular guillotine? Cell Death Differ. **6**:497–507.
3. **Broker, L. E., C. Huisman, S. W. Span, J. A. Rodriguez, F. A. Kruyt, and G. Giaccone.** 2004. Cathepsin B mediated caspase-independent cell death induced by microtubule stabilizing agents in non-small cell lung cancer cells. Cancer Res. **64**:27–30.
4. **Broker, L. E., F. A. Kruyt, and G. Giaccone.** 2005. Cell death independent of caspases: a review. Clin. Cancer Res. **11**:3155–3162.
5. **Coelho, D., V. Holl, D. Weltin, T. Lacornerie, P. Magnenet, P. Dufour, and P. Bischoff.** 2000. Capase-3-like activity determines the type of cell death following ionizing radiation in MOLT-4 human leukaemia cells. Br. J. Cancer **83**:642–649.
6. **Colino, J., and C. M. Snapper.** 2003. Two distinct mechanisms for induction of dendritic cell apoptosis in response to intact *Streptococcus pneumoniae*. J. Immunol. **171**:2345–2365.
7. **Cortes-Bratti, X., C. Karlsson, T. Lagergard, M. Thelestam, and T. Frisan.** 2001. The *Haemophilus ducreyi* cytolethal distending toxin induces cell cycle arrest and apoptosis via the DNA damage checkpoint pathways. J. Biol. Chem. **276**:5296–5302.
8. **Danial, N., and S. Korsmeyer.** 2004. Cell death: critical control points. Cell **116**:205–219.
9. **Elwell, C. A., and L. A. Dreyfus.** 2000. DNase I homologous residues in CdtB are critical for cytolethal distending toxin-mediated cell cycle arrest. Mol. Microbiol. **37**:952–963.
10. **Enoksson, M., J. D. Robertson, V. Gogvadze, P. Bu, A. Kropotov, B. Zhivotovsky, and S. Orrenius.** 2004. Caspase-2 permeabilizes the outer mitochondrial membrane and disrupts the binding of cytochrome *c* to anionic phospholipids. J. Biol. Chem. **279**:49575–49578.
11. **Essmann, F., H. Bantel, G. Totzke, I. H. Engels, B. Sinha, K. Schulze-Osthoff, and R. U. Janicke.** 2003. *Staphylococcus aureus* alpha-toxin-induced cell death: predominant necrosis despite apoptotic caspase activation. Cell Death Differ. **10**:1260–1272.
12. **Fink, S. L., and B. T. Cookson.** 2005. Apoptosis, pyroptosis, and necrosis: mechanistic description of dead and dying eukaryotic cells. Infect. Immun. **73**:1907–1916.
13. **Foghsgaard, L., D. Wissing, D. Mauch, U. Lademann, L. Bastholm, M. Boes, F. Elling, M. Leist, and M. Jaattela.** 2001. Cathepsin B acts as a dominant execution protease in tumor cell apoptosis induced by tumor necrosis factor. J. Cell Biol. **153**:999–1010.
14. **Fuhlbrigge, R. C., S. M. Fine, E. R. Unanue, and D. D. Chaplin.** 1988. Expression of membrane interleukin 1 by fibroblasts transfected with murine pro-interleukin 1 alpha cDNA. Proc. Natl. Acad. Sci. USA **85**:5649–5653.
15. **Guerra, L., K. Teter, B. N. Lilley, B. Sternerlow, R. K. Holmes, H. L. Ploegh, K. Sandvig, M. Thelestam, and T. Frisan.** 2005. Cellular internalization of cytolethal distending toxin: a new end to a known pathway. Cell. Microbiol. **7**:921–934.
16. **Hayashi, T., I. Hayashi, T. Shinohara, Y. Morishita, H. Nagamura, Y. Kusunoki, K. Kyoizumi, T. Seyama, and K. Nakachi.** 2004. Radiation-induced apoptosis of stem/progenitor cells in human umbilical cord blood is associated with alterations in reactive oxygen and intracellular pH. Mutat. Res. **556**:83–91.
17. **Heywood, W., B. Henderson, and S. P. Nair.** 2005. Cytolethal distending toxin: creating a gap in the cell cycle. J. Med. Microbiol. **54**:207–216.
18. **Hirsch, T., P. Marchetti, S. A. Susin, B. Dallaporta, N. Zamzami, I. Marzo, M. Geuskens, and G. Kroemer.** 1997. The apoptosis-necrosis paradox: apoptogenic proteases activated after mitochondrial permeability transition determine the mode of cell death. Oncogene **15**:1573–1582.
19. **Hockenbery, D., G. Nunez, C. Milliman, R. D. Schreiber, and S. J. Korsmeyer.** 1990. Bcl-2 is an inner mitochondrial membrane protein that blocks programmed cell death. Nature **348**:334–336.
20. **Jaattela, M., and J. Tschopp.** 2003. Capspase-independent cell death in T lymphocytes. Nat. Immunol. **4**:416–423.
21. **Jiang, X., and X. Wang.** 2004. Cytochrome *c*-mediated apoptosis. Annu. Rev. Biochem. **73**:87–106.

22. **Kadenbach, B., S. Arnold, I. Lee, and M. Huttermann.** 2003. The possible role of cytochrome *c* oxidase in stress-induced apoptosis and degenerative diseases. Biochim. Biophys. Acta **1655**:400–408.
23. **Kroemer, G., and S. J. Martin.** 2005. Caspase-independent cell death. Nat. Med. **11**:725–730.
24. **Kuida, K., T. S. Zheng, S. Na, C. Kuan, D. Yang, H. Karasuyama, P. Rakic, and R. A. Flavell.** 1996. Decreased apoptosis in the brain and premature lethality in CPP32-deficient mice. Nature **384**:368–372.
25. **Lara-Tejero, M., and J. E. Galan.** 2000. A bacterial toxin that controls cell cycle progression as a deoxyribonuclease I-like protein. Science **290**:354–357.
26. **Leist, M., and M. Jaattela.** 2001. Four deaths and a funeral: from caspases to alternative mechanisms. Nat. Rev. Mol. Cell. Biol. **2**:589–598.
27. **Martinon, F., and J. Tschopp.** 2004. Inflammatory caspases: linking an intracellular innate immune system to autoinflammatory diseases. Cell **117**: 561–574.
28. **Nishikubo, S., M. Ohara, M. Ikura, K. Katayanagi, T. Fujiwara, H. Komatsuzawa, H. Kurihara, and M. Sugai.** 2006. Single nucleotide polymorphism in the cytolethal distending toxin B gene confers heterogeneity in the cytotoxicity of *A. actinomycetemcomitans*. Infect. Immun. **74**:7014–7020.
29. **Nishikubo, S., M. Ohara, Y. Ueno, M. Ikura, H. Kurihara, H. Komatsuzawa, E. Oswald, and M. Sugai.** 2003. An N-terminal segment of the active component of the bacterial genotoxin cytolethal distending toxin B (CDTB) directs CDTB into the nucleus. J. Biol. Chem. **278**:50671–50681.
30. **Nougayrede, J. P., F. Taieb, J. De Rycke, and E. Oswald.** 2005. Cyclomodulins: bacterial effectors that modulate the eukaryotic cell cycle. Trend Microbiol. **13**:103–110.
31. **Ohara, M., T. Hayashi, Y. Kusunoki, M. Miyauchi, T. Takata, and M. Sugai.** 2004. Caspase-2 and caspase-7 are involved in cytolethal distending toxin-induced apoptosis in Jurkat and MOLT-4 T-cell lines. Infect. Immun. **72**: 871–879.
32. **Ohara, M., E. Oswald, and M. Sugai.** 2004. Cytolethal distending toxin: a bacterial bullet targeted to nucleus. J. Biochem. **136**:409–413.
33. **Qa'Dan, M., M. Ramsey, J. Daniel, L. M. Spyres, B. Safiejko-Mroczka, W. Ortiz-Leduc, and J. D. Ballard.** 2002. *Clostridium difficile* toxin B activates dual caspase-dependent and caspase-independent apoptosis in intoxicated cells. Cell. Microbiol. **4**:425–434.
34. **Ricci, J. E., R. A. Gottlieb, and D. R. Green.** 2003. Caspase-mediated loss of mitochondrial function and generation of reactive oxygen species during apoptosis. J. Cell Biol. **160**:65–75.
35. **Shenker, B. J., R. H. Hoffmaster, A. Zekavat, N. Yamaguchi, E. T. Lally, and D. Demuth.** 2001. Induction of apoptosis in human T cells by *Actinobacillus actinomycetemcomitans* cytolethal distending toxin is a consequence of G_2 arrest of the cell cycle. J. Immunol. **167**:435–441.
36. **Shimizu, S., T. Kanaseki, N. Mizushima, T. Mizuta, S. Arakawa-Kobayashi, C. B. Thompson, and Y. Tsujimoto.** 2004. A role of Bcl-2 family of proteins in non-apoptotic programmed cell death dependent on autophagy genes. Nat. Cell Biol. **6**:1221–1228.
37. **Shinohara, K., and H. Nakano.** 1993. Interphase death and reproductive death in X-irradiated MOLT-4 cells. Radiat. Res. **135**:197–205.
38. **Simond, R. J., R. Williams, T. R. Hirst, and N. A. Williams.** 2004. The B subunit of *Escherichia coli* heat-labile enterotoxin induced both caspase-dependent and -independent cell death pathways in $CD8^+$ T cells. Infect. Immun. **72**:5850–5857.
39. **Slots, J., H. S. Reynolds, and R. J. Genco.** 29. *Actinobacillus actinomycetemcomitans* in human periodontal disease: a cross-sectional microbiological investigation. Infect. Immun. **29**:1013–1020.
40. **Stoka, V., B. Turk, S. L. Schendel, T. H. Kim, T. Cirman, S. J. Snipas, L. M. Ellerby, D. Bredesen, H. Freeze, M. Abrahamson, D. Bromme, S. Krajewski, J. C. Reed, X. M. Yin, V. Turk, and G. S. Salvesen.** 2001. Lysosomal protease pathways to apoptosis: cleavage of bid, non-pro-caspases, is the most likely route. J. Biol. Chem. **276**:3149–3157.
41. **Strasser, A.** 2005. The role of BH-3only proteins in the immune system. Nat. Rev. Immunol. **5**:189–200.
42. **Sugai, M., T. Kawamoto, S. Y. Peres, Y. Ueno, H. Komatsuzawa, T. Fujiwara, H. Kurihara, H. Suginaka, and E. Oswald.** 1998. The cell cycle-specific growth-inhibitory factor produced by *Actinobacillus actinomycetemcomitans* is a cytolethal distending toxin. Infect. Immun. **66**:5008–5019.
43. **Susin, S. A., E. Daugas, L. Ravagnan, K. Samejima, N. Zamzami, M. Loeffler, P. Costantini, K. F. Ferri, T. Irinopoulou, M. C. Prevost, G. Brothers, T. W. Mak, J. Penninger, W. C. Earnshaw, and G. Kroemer.** 2000. Two distinct pathways leading to nuclear apoptosis. J. Exp. Med. **192**:571–579.
44. **Tinel, A., and J. Tschopp.** 2004. The PIDDosome, a protein complex implicated in activation of caspase-2 in response to genotoxic stress. Science **304**:843–846.
45. **Tsujimoto, Y.** 2003. Cell death regulation by the Bcl-2 protein family in the mitochondria. J. Cell Physiol. **195**:158–167.
46. **Ueno, Y., M. Ohara, T. Kawamoto, T. Fujiwara, H. Komatsuzawa, E. Oswald, and M. Sugai.** 2006. Biogenesis of the *Actinobacillus actinomycetemcomitans* cytolethal distending toxin holotoxin. Infect. Immun. **74**:3480–3487.
47. **Vanden Berghe, T., G. van Loo, X. Saelens, M. Van Gurp, G. Brouckaert, M. Kalai, W. Declercq, and P. Vandenabeele.** 2004. Differential signaling to apoptotic and necrotic cell death by FAS-associated death domain protein FADD. J. Biol. Chem. **279**:7925–7933.
48. **Vercammen, D., R. Beyaert, G. Denecker, V. Goossens, G. Van Loo, W. Declercq, J. Grooten, W. Fiers, and P. Vandenabeele.** 1998. Inhibition of caspases increases the sensitivity of L929 cells to necrosis mediated by tumor necrosis factor. J. Exp. Med. **187**:1477–1485.
49. **Woo, M., R. Hakem, M. S. Soengas, G. S. Duncan, A. Shahinian, D. Kagi, A. Hakem, M. McCurrach, W. Khoo, S. A. Kaufman, G. Senaldi, T. Howard, S. W. Lowe, and T. W. Mak.** 1998. Essential contribution of caspase 3/CPP32 to apoptosis and its associated nuclear changes. Genes Dev. **12**:806–819.
50. **Yamamoto, K., K. Tominaga, M. Sukedai, T. Okinaga, K. Iwanaga, T. Nishihara, and J. Fukuda.** 2004. Delivery of cytolethal distending toxin B induces cell cycle arrest and apoptosis in gingival squamous cell carcinoma in vitro. Eur. J. Oral Sci. **112**:445–451.
51. **Yu, L., A. Alva, H. Su, P. Dutt, E. Freundt, S. Welsh, E. H. Baehrecke, and M. J. Lenardo.** 2004. Regulation of an ATG7-beclin 1 program of autophagic cell death by caspase-8. Science **304**:1500–1502.
52. **Yuan, J. Y., and H. R. Horvitz.** 1990. The *Caenorhabditis elegans* genes *ced*-3 and *ced*-4 act cell autonomously to cause programmed cell death. Dev. Biol. **138**:33–41.

Editor: V. J. DiRita

Published in final edited form as:
Adv Exp Med Biol. 2008 ; 630: 19–34.

Adaptation to Estradiol Deprivation Causes Up-Regulation of Growth Factor Pathways and Hypersensitivity to Estradiol in Breast Cancer Cells

Richard J. Santen*, **Robert X. Song**, **Shigeru Masamura**, **Wei Yue**, **Ping Fan**, **Tetsuya Sogon**, **Shin-ichi Hayashi**, **Kei Nakachi**, and **Hidtek Eguchi**

Abstract

Deprivation of estrogen causes breast tumors in women to adapt and develop enhanced sensitivity to this steroid. Accordingly, women relapsing after treatment with oophorectomy, which substantially lowers estradiol for a prolonged period, respond secondarily to aromatase inhibitors with tumor regression. We have utilized in vitro and in vivo model systems to examine the biologic processes whereby Long Term Estradiol Deprivation (LTED) causes cells to adapt and develop hypersensitivity to estradiol. Several mechanisms are associated with this response including up-regulation of ERα and the MAP kinase, PI-3-kinase and mTOR growth factor pathways. ERα is 4–10 fold up-regulated as a result of demethylation of its C promoter, is nuclear receptor then co-opts a classical growth factor pathway using SHC, Grb-2 and Sos. is induces rapid nongenomic effects which are enhanced in LTED cells.

The molecules involved in the nongenomic signaling process have been identified. Estradiol binds to cell membrane-associated ERα which physically associates with the adaptor protein SHC and induces its phosphorylation. In turn, SHC binds Grb-2 and Sos which results in the rapid activation of MAP kinase. These nongenomic effects of estradiol produce biologic effects as evidenced by Elk-1 activation and by morphologic changes in cell membranes. Additional effects include activation of the PI-3-kinase and mTOR pathways through estradiol-induced binding of ERα to the IGF-1 and EGF receptors.

A major question is how ERα locates in the plasma membrane since it does not contain an inherent membrane localization signal. We have provided evidence that the IGF-1 receptor serves as an anchor for ERα in the plasma membrane. Estradiol causes phosphorylation of the adaptor protein, SHC and the IGF-1 receptor itself. SHC, after binding to ERα, serves as the "glue" which tethers ERα to SHC binding sites on the activated IFG-1 receptors. Use of siRNA methodology to knock down SHC allows the conclusion that SHC is needed for ERα to localize in the plasma membrane.

In order to abrogate growth factor induced hypersensitivity, we have utilized a drug, farnesylthiosalicylic acid, which blocks the binding of GTP-Ras to its membrane acceptor protein, galectin 1 and reduces the activation of MAP kinase. We have shown that this drug is a potent inhibitor of mTOR and this provides the major means for inhibition of cell proliferation. The concept of "adaptive hypersensitivity" and the mechanisms responsible for this phenomenon have important clinical implications. The efficacy of aromatase inhibitors in patients relapsing on tamoxifen could be explained by this mechanism and inhibitors of growth factor pathways should reverse the hypersensitivity phenomenon and result in prolongation of the efficacy of hormonal therapy for breast cancer.

*Corresponding Author: Richard J. Santen—Division of Endocrinology and Metabolism, University of Virginia Health Sciences Center, Charlottesville, Virginia, USA. Email: rjs5y@virginia.edu.
Innovative Endocrinology of Cancer, edited by Lev M. Berstein and Richard J. Santen.

Introduction

Cancer cells adapt in response to the pressure exerted upon them by various hormonal treatments. Ultimately, this process of adaptation renders them insensitive to hormonal therapy. In patients, clinical observations suggest that long term deprivation of estradiol causes breast cancer cells to develop enhanced sensitivity to the proliferative effects of estrogen. Premenopausal women with advanced hormone dependent breast cancer experience objective tumor regressions in response to surgical oophorectomy which lowers estradiol levels from mean levels of approximately 200 pg/ml to 10 pg/ml.[1] After 12–18 months on average, tumors begin to regrow even though estradiol levels remain at 10 pg/ml. Notably tumors again regress upon secondary therapy with aromatase inhibitors which lower estradiol levels to 1–2 pg/ml. These observations suggest that tumors develop hypersensitivity to estradiol as demonstrated by the fact that untreated tumors require 200 pg/ml of estradiol to grow whereas tumors regrowing after oophorectomy require only 10 pg/ml. We have shown in prior studies that up-regulation of growth factor pathways contributes to the phenomenon of hypersensitivity.[2–10] Ultimately these tumors adapt further and grow exclusively in response to growth factor pathways and do not require estrogens for growth.

In order to provide direct proof that hypersensitivity does develop and to study the mechanisms involved, we have utilized cell culture and xenograft models of breast cancer as experimental tools.[5,8,9,11–13]

Phenomenon of Hypersensitivity: Mechanisms and Pathways

To induce hypersensitivity, wild type MCF-7 cells require culturing over a 6–24 month period in estrogen-free media to mimic the effects of ablative endocrine therapy such as induced by surgical oophorectomy or aromatase inhibitors.[11,12] is process involves Long Term Estradiol Deprivation and the adapted cells are called by the acronym, LTED cells. As evidence of hypersensitivity, a three log lower concentration of estradiol can stimulate proliferation of LTED cells compared to wild type MCF-7 cells (Fig. 1A).[7] We reasoned that the development of hypersensitivity could involve modulation of the genomic effects of estradiol acting on transcription, nongenomic actions involving plasma membrane related receptors, cross talk between growth factor and steroid hormone stimulated pathways, or interactions among these various effects.[5,7–9,11–13]

We initially postulated that enhanced receptor mediated transcription of genes related to cell proliferation might be involved. Indeed, the levels of ERα increased 4–10 fold during long term estradiol deprivation.[11] The up-regulation of ER alpha results from demethylation of promoter A and C of the estrogen receptor (Fig. 1B and 1C). The transcripts stimulated by this promoter increase by 149 fold and the DNA of this segment exhibits a marked increase in demethylation. [13A]We initially reasoned that the up-regulation of ERα would directly result in hypersensitivity to estradiol (E_2). Accordingly, to directly examine whether enhanced sensitivity to E_2 in LTED cells occurred at the level of ER mediated transcription, we quantitated the effects of estradiol on transcription in LTED and in wild type MCF-7 cells. As transcriptional readouts, we measured the effect of E_2 on progesterone receptor (PgR) and pS2 protein concentrations and on ERE-CAT reporter activity (Fig. 2A–F).[9,13] We observed no shift to the left in estradiol dose response curves (the end point utilized to detect hypersensitivity) for any of these responses (i.e., PgR, pS2, CAT activity) when comparing LTED with wild type MCF-7 cells. On the other hand, basal levels (i.e., no estrogen added) of transcription of three ER/ERE related reporter genes were greater in LTED than in wild type MCF-7 cells (Fig. 2D–F).[13]

To interpret these data, we used the classic definition for hypersensitivity, namely a significant shift to the left in the dose causing 50% of maximal stimulation. Accordingly, these data suggest

that hypersensitivity of LTED cells to the proliferative effects of estradiol does not occur primarily at the level of ER-mediated gene transcription (Fig. 2A–C) but may be influenced by the higher rates of maximal transcription (Fig. 2D–F).

We next considered that adaptation might involve dynamic interactions between pathways utilizing steroid hormones and those involving MAP kinase and PI-3-kinase for growth factor signaling (Fig. 3A).[5,7–9,11–16] Our initial approach demonstrated that basal levels of MAP kinase were elevated in LTED cells in vitro (Fig. 2B, top panel) and in xenografts (data not shown) and were inhibited by the pure antiestrogen, fulvestrant.[8,11]

We further demonstrated that activated MAP kinase is implicated in the enhanced growth of LTED cells since inhibitors of MAP kinase such as PD98059 or U-0126 block the incorporation of tritiated thymidine into DNA.[7] To demonstrate proof of the principle of MAP kinase participation, we stimulated activation of MAP kinase in wild type MCF-7 cells by administering TGFα (data not shown). Administration of TGFα caused a two log shift to the left in the ability of estradiol to stimulate the growth of wild type MCF-7 cells. To demonstrate that this effect was related specifically to MAP kinase and not to a nonMAP kinase mediated effect of TGF alpha, we co-administered PD 98059. Under these circumstances, the two log left shift in estradiol dose response, returned back to the baseline dose response curve.[7] As further evidence of the role of MAP kinase, we administered U-0126 to LTED cells and examined its effect on level of sensitivity to estradiol. is agent partially shifted dose response curves to the right by approximately one-half log (data not shown).

While an important component, MAP kinase did not appear to be solely responsible for hypersensitivity to estradiol. Blockade of this enzyme did not completely abrogate hypersensitivity. Accordingly, we examined the PI-3-kinase pathway to determine if it was up-regulated in LTED cells as well (Fig. 3B) and examined several signaling molecules downstream from this regulatory kinase.[16] We determined that LTED cells exhibit an enhanced activation of AKT (Fig. 3B, second panel), P70 S6 kinase (Fig. 3B, third panel) and PHAS-1/4E BP-1 (Fig. 3B, fourth panel; see also below).[16] Dual inhibition of PI-3-kinase with Ly 294002 (specific PI-3-kinase inhibitor) and MAP kinase with U-0126 shifted the level of sensitivity to estradiol more dramatically: more than two logs to the right (Fig. 3C).[7]

One possible mechanism to explain the activation of MAP kinase would be through nongenomic effects of estrogen acting via ERα located in or near the cell membrane.[17–19] We postulated that membrane associated ERα might utilize a classical growth factor pathway to transduce its effects in LTED cells. The adaptor protein SHC represents a key modulator of tyrosine kinase activated peptide hormone receptors.[14–15,20] Upon receptor activation and auto-phosphorylation, SHC binds rapidly to specific phosphotyrosine residues of receptors through its PTB or SH2 domain and becomes phosphorylated itself on tyrosine residues of the CH domain.[14,15] The phosphorylated tyrosine residues on the CH domain provide the docking sites for the binding of the SH2 domain of Grb2 and hence recruit SOS, a guanine nucleotide exchange protein. Formation of this adapter complex allows Ras activation via SOS, leading to the activation of the MAPK pathway.[20]

We postulated that estrogen deprivation might trigger activation of a nongenomic, estrogen-regulated, MAP kinase pathway which utilizes SHC.[14–15,20–22] We employed MAP kinase activation as an endpoint with which to demonstrate rapid nongenomic effects of estradiol (Fig. 4A). The addition of E_2 stimulated MAP kinase phosphorylation in LTED cells within minutes. The increased MAP kinase phosphorylation by E_2 was time and dose-dependent, being greatly stimulated at 15 min and remaining elevated for at least 30 min. Maximal stimulation of MAP kinase phosphorylation was at 10^{-10} M of E_2.

We then examined the role of peptides known to be involved in growth factor signaling pathways that activate MAP kinase. SHC proteins are known to couple tyrosine kinase receptors to the MAPK pathway and activation of SHC involves the phosphorylation of SHC itself.[20–22] To investigate if the SHC pathway was involved in the rapid action of estradiol in LTED cells, we immunoprecipitated tyrosine phosphorylated proteins and tested for the presence of SHC under E_2 treatment. E_2 rapidly stimulated SHC tyrosine phosphorylation in a dose and time dependent fashion with a peak at 3 minutes.[20] The pure estrogen receptor antagonist, fulvestrant, blocked E_2-induced SHC and MAPK phosphorylation at 3 min and 15 min respectively. To demonstrate that the classical ER alpha mediated this response, we transfected a siRNA against ER alpha and showed down-regulation of this receptor and also abrogated the effect of estradiol to rapidly enhance MAP kinase activation. The time frame suggests that SHC is an upstream component in E_2-induced MAPK activation.

We reasoned that the adapter protein SHC may directly or indirectly associate with ERα in LTED cells and thereby mediate E_2-induced activation of MAP kinase. We considered this likely in light of recent evidence regarding ERα membrane localization.[23–25] To test this hypothesis, we immunoprecipitated SHC from nonstimulated and E_2-stimulated LTED cells and then probed immunoblots with anti-ERα antibodies. Our data showed that the ERα/SHC complex pre-existed before E_2 treatment and E_2 time-dependently increased this association.[20] In parallel with SHC phosphorylation, we observed a maximally induced association between ERα and SHC at 3 min (data not shown). MAP kinase pathway activation by SHC requires SHC association with the adapter protein Grb2 and then further association with SOS. By immunoprecipitation of Grb2 and detection of both SHC and SOS, we demonstrated that the SHC-Grb2-SOS complex constitutively existed at relatively low levels in LTED cells, but was greatly increased by treatment of cells with 10^{-10} M E_2 for 3 min.[20]

After the demonstration of protein-protein interactions, we wished to provide evidence that these biochemical steps resulted in biologic effects. Accordingly, we evaluated the role of estrogen activated MAP kinase on the function of the transcription factor, Elk-1. When activated, Elk-1 serves as a down stream mediator of cell proliferation. The phosphorylation of Elk1 by MAPK can up-regulate its transcriptional activity through phosphorylation. By cotransfection of LTED cells with both GAL4-Elk and its reporter gene GAL4-luc,[26,27] we were able to show that E_2 dose-dependently increased Elk-1 activation at 6 hours as shown by luciferase assay (Fig. 4B).[20]

We also wished to demonstrate biologic effects on cell morphology. To examine E_2 effects on reorganization of the actin cytoskeleton, we visualized the distribution of F-actin by phalloidin staining and also redistribution of the ERα localization in LTED and MCF-7 cells (data not shown).[20] Untreated MCF-7 cells expressed low actin polymerization and a few focal adhesion points. After E_2 stimulation, in contrast, the cytoskeleton underwent remodeling associated with formation of cellular ruffles, lamellipodia and leading edges, alterations of cell shape and loss of mature focal adhesion points. A sub-cellular redistribution of ERα to these dynamic membranes upon E_2 stimulation represented another important feature. The ER antagonist ICI 182 780 at 10^{-9} M blocked E_2-induced ruffle formation as well as redistribution of ERα to the membrane with little effect by itself. Therefore, these studies further demonstrated the rapid action of E2 with respect to dynamic membrane alterations in LTED cells.

A key unanswered question was how the ER could localize in the plasma membrane when it does not contain membrane localization motifs. We postulated that the IGF-1-receptor and SHC might be involved in this process (Fig. 5A).[28] A series of studies by other investigators suggested that ERα and the IGF-1 receptor might interact.[28] We tested the model that estradiol caused binding of SHC to ERα but also caused phosphorylation of the IGF-1 receptor. In this way, SHCwould serve as the "glue" which would tether ER alpha to the plasma membrane

where it would bind to the SHC acceptor site. To assess this possibility, we immunoprecipitated IGF-1 receptors before and after addition of estradiol. is caused SHC to bind to the IFG-1 receptor (Fig. 5C) and caused the IGF-1 receptor to become phosphorylated (Fig. 5B,C). In order to prove a causal effect for this role of SHC, we utilized an siRNA methodology to knock down SHC and showed that this prevented ERα from binding to the IGF-1 receptor.[28] As further evidence, we conducted confocal microscopy experiments to show that knockdown of SHC prevented ERα from localizing in the plasma membrane (data not shown).[29]

Ellis Levin and colleagues recently showed that ER alpha must be palmitylated before it can localize in the plasma membrane.[29A] Although speculative, we postulate that ER alpha requires palmitylation to travel to the plasma membrane but activated SHC serves to tether it to the membrane via IGF-1-R. In contrast to our previous concept that SHC serves as the "bus" to carry ER alpha to the membrane, we now postulate that SHC is the "glue" that tethers ER alpha there after binding to the IGF-1-R. Further studies will be necessary to dissect out each component of these interactions and their biologic relevance.

From the data reviewed, we conclude that membrane related ERα plays a role in cell proliferation and in activation of MAP kinase. It appeared likely then that LTED cells might exhibit enhanced functionality of the membrane ERα system. As evidence of this, we examined the ability of estradiol to cause the phosphorylation of SHC in wild type and MCF-7 cells and also to cause association of SHC with the membrane ERα. We demonstrated a marked enhancement of both of these processes in LTED as opposed to wild type cells. Considering all of these data together, it is still not clear at the present time what is responsible for enhancement of the nongenomic ERα mediated process.

If adaptive hypersensitivity results from the up-regulation of growth factor pathways, an inhibitor of MAP kinase and downstream PI-3-kinase pathways could be important in abolishing hypersensitivity and in inhibiting cell proliferation. We had been studying the effects of a MAP kinase inhibitor, farnesylthiosalicylic acid (FTS), which has been shown to block proliferation of LTED cells. is agent interferes with the binding of GTP-Ras to its acceptor site in the plasma membrane, a protein called galectin 1.[30] While examining its downstream effects, we have shown that this agent is also a potent inhibitor of phosphoinositol-3-kinase (PI-3-kinase). We postulated that an agent which blocks not only the MAP kinase pathway but also downstream actions of the PI-3-kinase pathway might be ideal to inhibit hypersensitivity. Accordingly, we have intensively studied the effects of FTS on mTOR.

The mammalian target of rapamycin, mTOR, is a Ser/r protein kinase involved in the control of cell growth and proliferation.[31] One of the best characterized substrates of mTOR is PHAS-1 (also called 4E-BP1).[32,33] PHAS-I/4E-BP1 binds to eIF4E and represses cap-dependent translation by preventing eIF4E from binding to eIF4G.[32,33] When phosphorylated by mTOR, PHAS-I/4E-BP1 dissociates from eIF4E, allowing eIF4E to engage eIF4G, thus increasing the formation of the eIF4F complex needed for the proper positioning of the 40S ribosomal subunit and for efficient scanning of the 5′-UTR.[31] In cells, mTOR is found in mTORC1, a complex also containing raptor, a newly discovered protein of 150kDa. It has been proposed that raptor functions in TORC1 as a substrate-binding subunit which presents PHAS-I/4E-BP1 to mTOR for phosphorylation.[31,32] Our results suggest that FTS inhibits phosphorylation of the mTOR effectors, PHAS-I/4E-BP1 and S6K1, in response to estrogen stimulation of breast cancer cells.[2]

To investigate the effects of FTS on mTOR function, we utilized 293T cells and monitored changes in the phosphorylation of PHAS-I/4E-BP1.[2] Incubating cells with increasing concentrations of FTS decreased the phosphorylation of PHAS-I/4E-BP1, as evidenced by a